JGR Biogeosciences

RESEARCH ARTICLE
10.1029/2022JG007113

Estimating Net Carbon and Greenhouse Gas Balances of Potato and Pea Crops on a Conventional Farm in Western Canada

Ningyu Quan[1], Sung-Ching Lee[2,3], Chitra Chopra[1], Zoran Nesic[1], Paula Porto[1], Patrick Pow[1], Rachhpal S. Jassal[1], Sean Smukler[1], Maja Krzic[1,4], Sara H. Knox[2], and T. Andrew Black[1]

[1]Faculty of Land and Food Systems, University of British Columbia, Vancouver, BC, Canada, [2]Department of Geography, University of British Columbia, Vancouver, BC, Canada, [3]Department Biogeochemical Integration, Max Planck Institute for Biogeochemistry, Jena, Germany, [4]Faculty of Forestry, University of British Columbia, Vancouver, BC, Canada

Abstract Quantifying the emissions of the three main biogenic greenhouse gases (GHGs), carbon dioxide (CO_2), nitrous oxide (N_2O) and methane (CH_4), from agroecosystems is crucial. In this study continuous measurements of N_2O, and CH_4 emissions from potato and pea crops in southwest British Columbia, Canada were made using the eddy-covariance (EC) technique. Flux footprint analysis, coupled with EC and manual nonsteady state chamber measurements, was used to address the spatial heterogeneity resulting from the field edge at the study site. Flux footprint corrections had a larger effect on N_2O fluxes than CO_2 fluxes because of a more pronounced difference in N_2O fluxes between the crop and edge areas. After flux footprint corrections, the potato and pea crops were both weak CO_2 sinks with annual net ecosystem exchange values of -57 ± 9 and -97 ± 16 g C m^{-2} yr^{-1}, respectively. However, after taking carbon (C) export via crop harvest and C import via seeding into account, the potato crop shifted to being a moderate C source of 284 ± 55 g C m^{-2} yr^{-1}, while the pea crop became near C neutral, sequestering only 30 ± 26 g C m^{-2} yr^{-1}. Annual GHG balances, quantified by converting N_2O and CH_4 to CO_2 equivalents as pulse emissions using respective global warming potentials on a 100-year timescale, were 417 ± 88 and 152 ± 106 g CO_2e m^{-2} yr^{-1} for the potato and pea crops, respectively, with N_2O contributing the largest proportion to annual total GHG balances and outweighing the CO_2 uptake from the atmosphere.

Plain Language Summary To better mitigate climate change, quantifying the emissions of the three main biogenic greenhouse gases (GHGs), carbon dioxide (CO_2), nitrous oxide (N_2O) and methane (CH_4), from agroecosystems is critical. Therefore, in this study we made continuous half-hourly measurements of CO_2, N_2O, and CH_4 emissions from potato and pea crops in southwest British Columbia, Canada using micrometeorological instrumentation installed at the field edge. To correct for the effects of the field edge on the micrometeorological measurements, we used supplementary chamber measurements and a footprint model. This enabled us to estimate the actual GHG budgets of the study crop areas. The correction had a larger effect on N_2O fluxes than CO_2 fluxes because of a more pronounced difference in N_2O fluxes between the crop and edge areas. Both crops sequestered CO_2 on an annual basis. However, after taking carbon (C) export via crop harvest and C import via seeding into account, the potato crop shifted to being a moderate C source while the pea crop became near C neutral. Even though CH_4 emissions were low, substantial N_2O emissions outweighed the CO_2 uptake from the atmosphere by both crops, resulting in both being GHG sources.

Key Points:

- Combining eddy-covariance and flux-chamber data with flux analysis allowed estimation of actual greenhouse gas fluxes from crop fields
- Including export (harvesting) and import (seeding), peas were near carbon neutral while potatoes were a moderate carbon source
- For both potato and pea crops, nitrous oxide contributed the largest proportion of the annual total greenhouse gas emissions

Supporting Information:

Supporting Information may be found in the online version of this article.

Correspondence to:

S.-C. Lee,
sclee@bgc-jena.mpg.de

Citation:

Quan, N., Lee, S.-C., Chopra, C., Nesic, Z., Porto, P., Pow, P., et al. (2023). Estimating net carbon and greenhouse gas balances of potato and pea crops on a conventional farm in western Canada. *Journal of Geophysical Research: Biogeosciences*, *128*, e2022JG007113. https://doi.org/10.1029/2022JG007113

Received 28 JUL 2022
Accepted 22 FEB 2023

Author Contributions:

Conceptualization: Rachhpal S. Jassal, Sean Smukler, Maja Krzic, T. Andrew Black
Data curation: Zoran Nesic
Formal analysis: Ningyu Quan, Sung-Ching Lee, Chitra Chopra
Funding acquisition: Rachhpal S. Jassal, Sean Smukler, Maja Krzic, T. Andrew Black
Investigation: Ningyu Quan, Sung-Ching Lee, Paula Porto, Patrick Pow
Methodology: Zoran Nesic, Rachhpal S. Jassal, T. Andrew Black

1. Introduction

As the global population expands rapidly, there is a surge in global food demand. A 100%–110% increase in global crop demand from 2005 to 2050 has been predicted (Tilman et al., 2011). Using a more recent projection with 2010 as a baseline, the total global food demand is expected to increase by up to 56% in 2050 when considering climate change impacts (van Dijk et al., 2021). This drastic increase has exerted considerable pressures on agroecosystems (Kanianska et al., 2016). While agroecosystems play a critical role in global food supply, they also release greenhouse gases (GHGs) into the atmosphere contributing to climate change (Hartmann et al., 2013). Furthermore, global climate change, involving changes in precipitation and an increased frequency of extreme weather events that are likely to occur during this century (Canadell et al., 2021; Seneviratne et al., 2012), presents a significant challenge to agricultural production.

Project Administration: Sean Smukler, Maja Krzic, T. Andrew Black
Resources: T. Andrew Black
Supervision: Ningyu Quan, Sung-Ching Lee, Rachhpal S. Jassal, Sean Smukler, Sara H. Knox, T. Andrew Black
Visualization: Ningyu Quan, Sung-Ching Lee
Writing – original draft: Ningyu Quan, Sung-Ching Lee
Writing – review & editing: Ningyu Quan, Sung-Ching Lee, Chitra Chopra, Zoran Nesic, Paula Porto, Patrick Pow, Rachhpal S. Jassal, Sean Smukler, Maja Krzic, Sara H. Knox, T. Andrew Black

Thus, quantification of the three main biogenic GHGs, carbon dioxide (CO_2), nitrous oxide (N_2O), and methane (CH_4), from agroecosystems is crucial in providing knowledge for climate-change related policy making (Maier et al., 2022).

In 2020, Canadian agricultural sector accounted for 8.2% of total national GHG emissions releasing 55 Mt CO_2 eq to the atmosphere, with a large proportion of the emissions (~40%) resulting from agricultural soils, and 75% of national N_2O emissions (Environment and Climate Change Canada, 2022). One of the main drivers of these emissions, based on inventory data, is the application of inorganic nitrogen fertilizers to agricultural soils in the Prairie Provinces (Environment and Climate Change Canada, 2022). In May 2015, Canada announced its intentions to reduce GHG emissions by 30% below 2005 levels by 2030 confirming its commitments in its Nationally Determined Contribution (NDC) to the Paris Agreement. This resulted in a considerable research directed toward mitigating GHG emissions generated by agricultural systems, but these studies have been largely limited to Ontario (Wagner-Riddle et al., 2007) and the Canadian Prairies including the provinces of Manitoba, Saskatchewan, and Alberta (Asgedom & Kebreab, 2011; Liebig et al., 2005; Rochette et al., 2018). Such efforts are greatly needed in other parts of Canada to allow the development of strategies to mitigate GHG emissions, while developing climate-change related policies.

In British Columbia (BC), GHG emissions in forage grass and silage corn fields have been monitored periodically using manual chambers (e.g., Bhandral et al., 2009; Bittman & Hunt, 2015; D. E. Hunt et al., 2016), and, recently, in a highbush blueberry (*Vacinium corymbosum* L.) field year-round with automated chambers (Shabtai Bittman, personal communication). Yet, field-scale, continuous, year-round measurements, needed to reliably quantify annual emissions from local high-value cropping systems, have been lacking.

The fertile soils in the Lower Fraser Valley (LFV) in BC allow for intensive arable cropping such as field vegetables and berries. Potatoes (*Solanum tuberosum* L.), as one of the main crops in the LFV, account for about 50% of BC's total area in potato production (British Columbia Agriculture & Food Climate Action Initiative, 2013), while peas (*Pisum sativum* L.) account for 7.8% of the total area of vegetables grown for harvest in BC (Statistics Canada, 2016) and are often planted following a potato crop in a typical crop rotation. Even though potatoes and peas are important crops in BC, no continuous measurements of GHG fluxes are available for those two crops in this region.

The eddy-covariance (EC) technique, an effective and widely-used micrometeorological technique, is used to determine half-hourly GHG fluxes at the landscape scale by measuring high-frequency fluctuations of vertical wind velocity and GHG concentrations above the field (Baldocchi, 2014). While the requirements of homogeneous surfaces and stationary conditions need to be met to conduct EC flux measurements, it must be recognized that some degree of spatial variability and inhomogeneity are inevitable over vegetated surfaces in most cases (Levy et al., 2020; Molodovskaya et al., 2011; Nagy et al., 2006). In such situations, flux chambers, as an important supplementary technique, can be used to determine localized soil GHG emissions from each contributing landscape component and to verify EC-integrated fluxes (Famulari et al., 2010; Schrier-Uijl et al., 2010; Waldo et al., 2019). Flux footprint (upwind source area contributing to the EC flux measurement) models have been used to compare GHG fluxes measured by point-scale chamber and landscape-scale EC systems when upscaling chamber fluxes (Christensen et al., 1996; Levy et al., 2020; Molodovskaya et al., 2011; Schrier-Uijl et al., 2010). Additionally, flux footprint models can be employed to make corrections for the field edge effect and estimate surface flux of each landscape component of the source area (Schmid, 1994).

In this study, continuous EC measurements of CO_2, N_2O, and CH_4 emissions from potato and pea fields (Figure 1) were made year-round in the LFV of BC, Canada. The EC flux footprint comprised cropped areas on both sides of the edge area comprising a farm road, machinery turn-around strip and a drainage ditch, so footprint analysis was combined with EC and chamber measurements of soil GHG fluxes to estimate the annual GHG budgets of the cropped areas. The objectives of this study were to:

1. Determine spatial and temporal variations in CO_2, N_2O, and CH_4 fluxes of potato and pea fields using EC and nonsteady state flux chamber techniques.
2. Combine flux measurements with a footprint modeling approach to obtain actual GHG fluxes of the crop fields from the EC-measured ecosystem-scale fluxes.
3. Quantify annual net carbon (C) and GHG balances of the study fields.

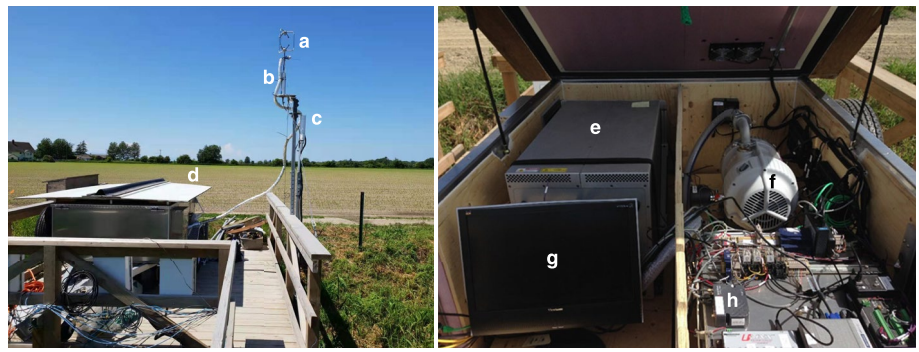

Figure 1. Photos of (a) the sonic anemometer, (b) air sampling inlet tubes of the infrared gas analyzer (IRGA) and laser spectrometer, (c) IRGA, (d) trailer with the laser spectrometer inside, (e) the laser spectrometer, (f) dry scroll vacuum pump for the laser spectrometer, (g) site computer, and (h) communication system for daily transmission of data to the lab.

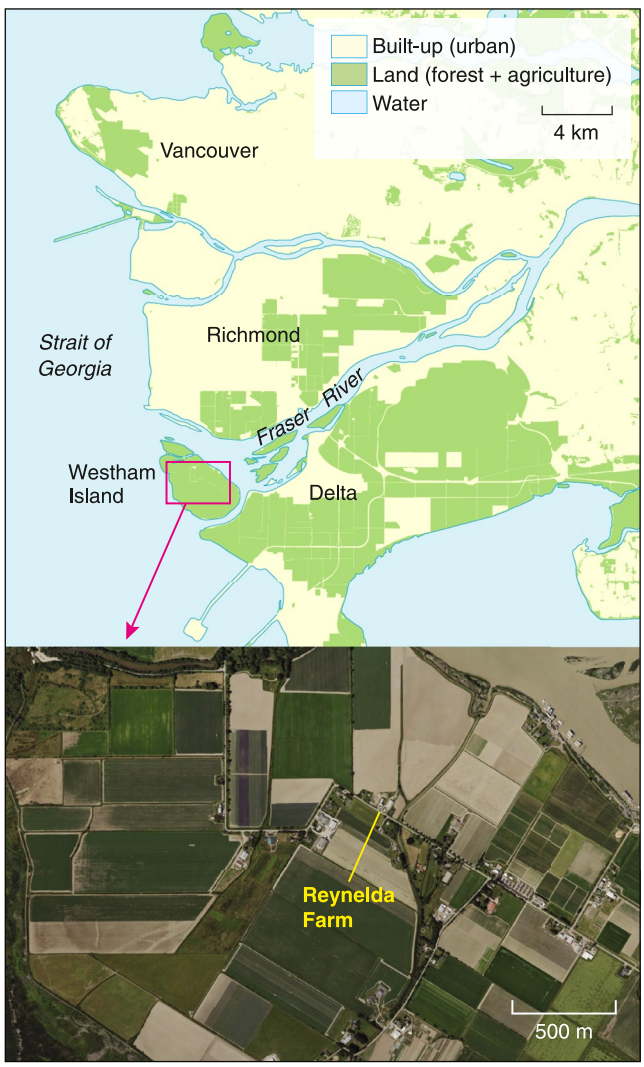

Figure 2. Reynelda Farm indicated by the yellow solid line is located on Westham Island, which is on the southwest edge of the Fraser River delta, BC, Canada.

2. Methods

2.1. The Study Site

The study site was located on Reynelda Farm (49°05′25.0″N, 123°09′47.9″W), a conventionally managed farm located on Westham Island, which is on the southwest edge of the Fraser River delta (Figure 2). This farm is typical of cropland in the area and was planted with potatoes, peas and silage corn during the study period in 2018 and 2019. The soils on the farm are Crescent Orthic Gleysol and Westham Rego Humic Gleysol, both naturally poorly drained and prone to ponding in the winter (Luttmerding, 1981). Our soil bulk density measurements on the ridge and furrow in the potato crop at the 0–7-cm depth were 1.27 and 1.50 g cm^{-3}, respectively. The texture of the topsoil is silt loam and the average pH of the top 15 cm of soil is 4.7 (Pow et al., 2020). The 30-year (1981–2010) climate record of the nearby weather station at Vancouver International Airport (YVR) (49°11′42.0″N, 123°10′55.0″W), 12 km north of the study site, indicated an average annual air temperature of 10.4°C, rainfall of 1152.8 mm, and snowfall of 38.1 cm (Environment and Climate Change Canada). A large proportion (~80%) of precipitation occurs between October and April, contributing to appreciable seasonal variability in the soil moisture conditions.

The experimental site mainly comprised three landscape components: a narrow drainage ditch (north-south oriented) with grass on its sides, a relatively bare soil strip on both sides, serving as a farm road (west side) and farm machinery turn-around area (east side), and crop fields on both sides of the ditch. For simplicity, both the ditch (water filled in the non-growing season) and bare soil strips are referred to the "edge area" in this study (Figure S1 in Supporting Information S1).

In 2018, potatoes (varieties Goldrush Russet and Satina) were grown in both west and east fields as fresh produce. Both fields were plowed using a John Deere 975 reversible plow to a depth of 0.40 m 14 days before planting. They were fertilized 2 days before and during planting (15 May 2018) with a total application of 110 kg N ha^{-1} as NH_4NO_3 fertilizer. In 2019, peas (variety Serge) were grown in the east field, while corn was grown in the west field. The pea field was disc harrowed 7–10 days before planting and broadcast fertilized with 34 kg N ha^{-1} of NH_4NO_3. Potato and pea canopy heights were steady at 0.45 and 0.35 m, respectively, during most of the growing season. After crop harvest, the aboveground biomass was left on the ground for both potatoes and peas.

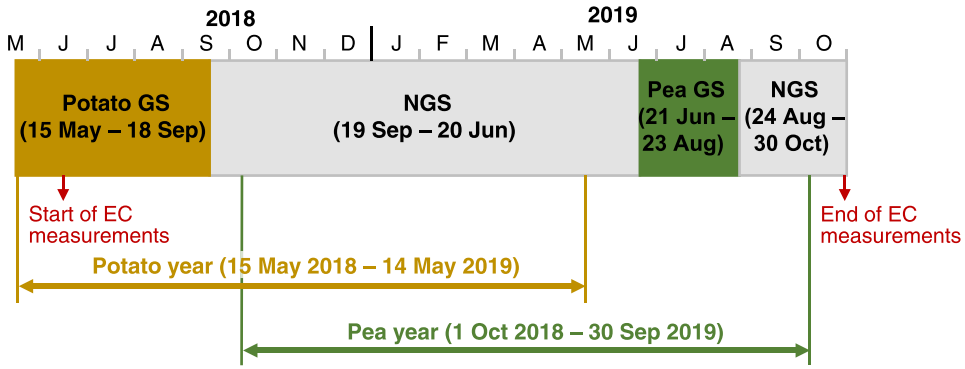

Figure 3. The timeline of the potato growing season (GS), the non-growing season (NGS) and the pea growing season (GS). The time periods of the EC measurements (20 June 2018–30 October 2019), the defined potato year and the defined pea year are indicated by red, brown and green arrows, respectively.

During the potato growing season (15 May 2018–18 September 2018) and non-growing season (19 September 2018–20 June 2019) (Figure 3), the west and east fields were managed in the same way. During the pea growing season (21 June 2019–23 August 2019) and non-growing season (24 August 2019–30 October 2019), the west and east fields were planted with corn and peas, respectively. Due to insufficient winds from the west field during the corn growing season and insufficient measurement height of EC tower (3 m) compared with the maximum height of corn (3.1 m), it was not possible to obtain a complete time series of GHG fluxes from the corn field and to make reliable estimates of GHG budgets. Therefore, the corn crop was not included in this study and the second production cycle is referred to as the pea year (Figure 3).

2.2. Field Instrumentation

2.2.1. Flux Tower Location

The EC mast was located on a wooden platform above the ditch (not always water-filled) in the middle of the edge area to avoid interference with regular farm operations. This had the benefit of having the EC tower between the two crop fields to receive upwind flux signals from both fields as wind direction changed from one field to the other during the crop growing season. The width of the edge area adjacent to the west and the east fields was 10 and 14 m, respectively. The width of the edge area adjacent to the east field was reduced to 6 m during the pea growing season since the farmer planted the peas without leaving a machinery turn around strip beside the ditch. All the soil and meteorological measurements were made in the edge area to avoid disturbance from farm operations.

2.2.2. Eddy-Covariance (EC) Measurements

Fluxes of CO_2, N_2O, and CH_4 were measured continuously from 20 June 2018 to 30 October 2019 at the field scale by the EC sensors installed on the mast at a fixed height of 3 m. It is important to note that GHG fluxes from the beginning of the potato growing season (15 May 2018) were not measured by the EC system due to delayed installation while chamber measurements were made. The EC system consisted of a three-dimensional sonic anemometer (R3-50, Gill Instruments Ltd., Lymington, UK), an enclosed-path infrared gas analyzer (IRGA) (LI-7200, LI-COR Inc., Lincoln, NE, USA) and an off-axis integrated cavity output spectrometer (model 913–1054, Los Gatos Research Inc., San Jose, CA, USA; hereafter "laser spectrometer") (Figure 1). The sonic anemometer measured the magnitudes of the three wind velocity components (u, v, w) and sonic temperature (T_{sonic}) at 20 Hz. The IRGA measured CO_2 (ρ_c) and water vapor (H_2O) densities in air (ρ_v) at 20 Hz. The laser spectrometer measured gas densities of N_2O (ρ_{N_2O}), CH_4 (ρ_{CH_4}), and ρ_v at 10 Hz. Both gas analyzers reported concentrations on a dry mole basis (i.e., mixing ratios) at the measurement frequency thus not requiring subsequent Webb-Pearman-Leuning (WPL) corrections (Webb et al., 1980).

Sample air was drawn through two separate air sampling inlets, one for the IRGA and the other for the laser spectrometer, positioned 15 cm below the center of the sonic anemometer array to avoid disturbance to the sonic measurements. The IRGA was mounted 2.5 m above the ground on the measurement mast and connected to a

1.3-m long and 4-mm inner-diameter air-sampling tube (Synflex 1300 Metal-Plastic composite tubing) (Eaton Corp. Inc., Beachwood, OH, USA) (flow rate of 15 L min^{-1}). A second Synflex air-sampling tube 3.8-m long and 4-mm inner diameter (flow rate of 20 L min^{-1}) running parallel to the first one was connected to the laser spectrometer, which was in an insulated water-proof box (2 m wide × 3 m long × 0.8 m high) mounted on a trailer (trailer top was 1.8 m above the soil surface). Temperature in the box was maintained at 35–36°C to ensure that the temperature in the laser spectrometer optical bench remained at 44.5 ± 0.1°C as recommended by the manufacturer. The air was drawn through the laser spectrometer by a dry scroll vacuum pump (XDS35i, Edwards Ltd., Burgess Hill, UK) at flow rate of 20 L min^{-1} (Figure 1). The cell pressure of the IRGA was maintained at −2.8 to −3.4 kPa below atmospheric pressure, while that of the laser spectrometer was maintained at 18.7 kPa (140 Torr) (as recommended by the manufacturers). The two sampling tubes were insulated and heated to 5–10°C above the ambient air temperature to reduce condensation inside the tubes. Before the sample air entered the IRGA and laser spectrometer, particulates were removed with a reusable 2-μm mesh 316-stainless steel filter (Swagelok Co., Solon, OH, USA) on the inlet, and a weekly manual replacement of the filters (after sonic bath cleaning) was performed to ensure adequate air flow in the tubing. Calibrations of the IRGA and laser spectrometer using a reference gas of known CO_2, N_2O, and CH_4 mixing ratios supplied by Environment and Climate Change Canada were conducted when necessary, based on the performance of the instruments, to ensure quality measurements. The zero offsets were determined using high purity (>99.998%) nitrogen gas.

Half-hourly EC fluxes were automatically calculated on the site computer using Matlab (The MathWorks Inc.). The calculated flux values were then transferred to the lab via cellular modem (Sierra Wireless RV50) on a daily basis. The real-time high-frequency data were backed up on a USB stick and manually transferred to a computer at the Biometeorology and Soil Physics Lab at University of British Columbia every week in case recalculations of half-hourly flux data were required (i.e., calculation procedure changes or interruptions on the site computer).

All half-hourly values of the three GHG fluxes were filtered for spikes (Humphreys et al., 2006) and non-stationarity. We also manually checked the half-hourly fluxes to remove suspect measurements. The detailed calculations and quality control can be found in Pow et al. (2020). In addition, the data with the friction velocity (u_*) less than 0.10 m s^{-1} were discarded. This threshold was determined by observing that nighttime EC-measured CO_2 fluxes remained relatively constant after u_* exceeded this value (Humphreys et al., 2006). To separate fluxes for the two crop fields, wind direction ranges of 210°–330° and 50°–130° were used to select flux data for the west and east crop fields, respectively (see Appendix A1 and Figure A1). These wind direction windows were based on the criteria that more than 60% of the total flux footprint contribution from the crop and the edge areas together should be met. This was intended not only to avoid effects of the area beyond the potato and pea crops but also to avoid too much data loss. During the 2019 growing season, peas were planted in the east field, so data were only selected for winds from 50° to 130°.

2.2.3. Climate and Energy Balance Measurements

A four-component net radiometer (CNR1, Kipp & Zonen, Delft, The Netherlands) mounted 0.7 m above the ground measured incoming shortwave (S_d), outgoing shortwave (S_u), incoming longwave (L_d) and outgoing longwave (L_u) radiation. One quantum sensor (LI-190, LI-COR Inc.) mounted at the 1-m height measured incoming photosynthetically active radiation (PAR). Precipitation (P) was measured using a tipping bucket rain gauge (TR-525M, Texas Electronics, Dallas, TX, USA) at the 1-m height. Air temperature (T_a) was measured at the 2.5-m height using a bare 75-μm type-E (chromel-constantan) thermocouple. Three copper-constantan thermocouples and three water content reflectometers (CS616, Campbell Scientific Inc. (CSI), Logan, UT, USA) were installed to measure soil temperature and soil volumetric water content, respectively, at depths of 5, 20 and 60 cm. Three soil heat flux plates (CN3, Middleton Solar, Melbourne, Australia) were installed at the 3-cm depth to measure the soil heat flux (G) on the edge area. Due to malfunctioning of the rain gauge at the site, P from January to March in 2019 was gap-filled using data from the nearby climate station at YVR. All the data were logged on the CR3000 datalogger (CSI) using a signal multiplexer (AM16/32B, CSI), and was output on a half-hourly average basis.

2.2.4. Chamber Measurements

Soil surface fluxes of CO_2, N_2O, and CH_4 from the edge area and the crop fields were measured manually every two weeks using a nonsteady state flux chamber from May 2018 to August 2019. The measurements had to be discontinued after August 2019 as the chamber gas analyzer failed and had to be sent back to the manufacturer

for repairs. Four opaque cylindrical PVC collars (i.d. 20 cm, height 15 cm) were installed on both sides of the EC tower, with the collars inserted approximately 5 cm into soil. Two of these collars were located in the edge area, with one collar in the edge of the east field and one in the edge of the west field. The other two were located in the crop field, with one being in the plant-row and the other being in the interrow. Existing vegetation that interfered with tight sealing of the chamber lid was cut to a level below the lid. Collars in the edge area were left in place for the entire study period while those in the field were temporarily removed for farm operations.

A portable Fourier Transform Infrared (FTIR) Spectrometer gas analyzer (Gasmet DX4040) (Gasmet Technologies Group, Helsinki, Finland) was paired with the chambers to measure soil surface fluxes of CO_2, N_2O, and CH_4 following the procedure described by Schiller and Hastie (1994). Teflon-® tubing (i.d. 4 mm; flow rate of 2–3 L min^{-1}) connected the metal lid to a silica gel container to remove excess moisture from the air stream. Air then passed through a 7-µm stainless steel filter before being drawn into the gas analyzer and then returned to the chamber.

All chamber measurements were made between 9:00 a.m. and 5:00 p.m. (PST). To ensure accurate gas flux estimation, the Gasmet readings of all the gases were verified for zero concentration level by flushing nitrogen gas through the system before each sampling campaign. The system was also tested for leakage in the laboratory the day before each campaign. While making measurements in the field on each sampling day, the FTIR was turned on for 5 min to warm up the gas analyzer and to stabilize background atmospheric gas concentrations before making measurements. Then the opaque lid was placed on the PVC collar for 6 min with 9 measurements made per minute. Ancillary measurements included collar air temperature (measured at the beginning, middle, and end of each cycle) and soil temperature (measured once per cycle at the 10-cm depth outside the collar) using a thermometer. Soil volumetric water content (0–7.6 cm depth) was once per cycle at three locations outside of the collar (within 30 cm) using a Fieldscout TDR 150 (Spectrum Technologies, Inc. Plainfield, IL) soil moisture meter with 7.6-cm long rods. The height of the collar above the soil surface at four different locations was measured and averaged to determine the volume of the chamber head space. The fluxes were determined by developing a linear relationship between the measured GHG mixing ratios and time since lid placement following Equation 1 in Christen et al. (2016). The CO_2 flux (or soil respiration) was used to approximate ecosystem respiration for the edge area. In summary, the chamber measurements were made to (a) gap-fill flux data during the period before the EC system was installed (refer to Section 2.3.1), and (b) provide fluxes from the edge area and hence allow us to calculate the actual crop field GHG fluxes (refer to Section 2.4.2).

2.3. Flux and Annual Balance Calculations

2.3.1. Flux Gap-Filling

After screening half-hourly EC data, valid half-hourly fluxes after all the quality controls for CO_2, N_2O, and CH_4 were 54%, 54%, and 56%, respectively, for the whole study period (i.e., including both potato and pea seasons). Gaps of an hour or less were filled by linear interpolation and longer gaps were filled using mean diurnal variation (MDV) over 5 to 14-day cycles (Falge et al., 2001; Nemitz et al., 2018).

To estimate net GHG balances of the crops using EC-measured fluxes, a complete time series of half-hourly chamber-measured GHG fluxes at the edge area was required (refer to Section 2.4). In the case of N_2O fluxes, chamber-measured N_2O fluxes from the edge area were gap-filled using a simple spline interpolation. The magnitude and fluctuations of the N_2O fluxes for the edge area were very small compared to those from the crop field. Thus, when the chamber gas analyzer failed during the pea non-growing season (i.e., 24 September 2019), we assumed N_2O emission from the edge area were the same as the previous year (i.e., 24 September 2018). Then we performed the same simple spline interpolation method between the two values (i.e., chamber-measured fluxes on 13 August 2019 and 24 September 2018) to obtain the complete time series of chamber-measured N_2O fluxes from the edge area. In the case of chamber-measured CO_2 fluxes of the edge area, the complete time series was obtained using an empirical relationship between manual chamber-measured CO_2 fluxes and soil temperature expressed as a logarithmic transformation of Equation 2. In the case of chamber-measured CH_4 fluxes, no gap-filling was applied as the fluxes were close to minimum detectable levels, that is, negligible.

As explained in Section 2.2.2, EC-measurements of GHG fluxes from the beginning of the potato growing season (15 May to 20 June 2018) were not made. However, chamber measurements from late May and early June indicated the response of the field to the fertilizer application and enabled us to estimate the GHG emissions during that period using linear interpolation.

2.3.2. Partitioning of Eddy Covariance Data

Net ecosystem exchange (NEE) was partitioned into two components as:

$$\mathrm{NEE} = -\mathrm{NEP} = R_e - \mathrm{GPP} \tag{1}$$

where NEE was equated to F_{CO_2} as changes in CO_2 storage in the air column beneath the EC measurement height were negligible considering the low EC measurement height (Montagnani et al., 2018). NEP is net ecosystem production, GPP is gross primary production, and R_e is ecosystem respiration. A negative NEE value indicates CO_2 uptake by the ecosystem from the atmosphere and a positive value indicates CO_2 release from the ecosystem to the atmosphere. The NEE partitioning procedure followed the standard FLUXNET Canada Research network (FCRN) protocol (i.e., nighttime-based partitioning method) using a moving window approach (Barr et al., 2004; Chen et al., 2009).

To investigate the effect of environmental variables on R_e and its estimation during daytime as well as gap-filling, a logarithmic transformation, $\ln R_e = A + BT_s$, which allows the assumption of normality and homoscedasticity to be met for linear least squares regression, was used to obtain the parameters in the exponential relationship between R_e and soil temperature (Humphreys et al., 2005):

$$R_e = R_{10} Q_{10}^{(T_s - 10)/10} \tag{2}$$

where R_{10} is the reference respiration rate at 10°C, Q_{10} is the relative increase in R_e for a 10°C increase in temperature and T_s is the soil temperature at the 5-cm depth.

2.3.3. Net Ecosystem Carbon and Greenhouse Gas Balances

Because EC measurements during the non-growing season following pea harvest were not completed, measurements in part of the previous non-growing season (1 October 2018–14 May 2019) were used in the calculation of the annual net ecosystem carbon balances (NECB, g C area^{-1} time^{-1}) and balances of GHGs (g CO_2e area^{-1} time^{-1}) of the pea crop. The timeline of the EC measurements and defined potato and pea years are shown in Figure 3. NECB was calculated using (Chapin et al., 2006; J. E. Hunt et al., 2016; Waldo et al., 2016):

$$\mathrm{NECB} = -\mathrm{NEE} + C_{\mathrm{import}} - C_{\mathrm{export}} \tag{3}$$

where C_{import} and C_{export} are C import as a result of seeding and organic fertilizer and export as a result of harvested biomass, respectively. Negative values of NECB indicate net loss of C from the field. As no organic fertilizer or amendments were applied, C_{import} values were estimated from the seeding rates of the potatoes and peas (3,440 kg wet matter ha^{-1}and 220 kg dry matter ha^{-1}, respectively). Using 78% water content of the seed potatoes and C content of 50% of the dry matter gave C_{import} values of 38 ± 8 and 11 ± 2 g C m^{-2} yr^{-1} for the potatoes and pea, respectively, assuming an uncertainty of ±20%. C_{export} was estimated using the fresh weight yields provided by the farmer and the typical C content in dry matter of potato tubers and peas (assumed to be 50%). The yield of potatoes (tubers) and peas (including pods) were 34.6 and 10.4 *t* wet matter ha^{-1}, respectively. Water contents of the tubers and peas were estimated to be 78% and 70%, respectively. The resulting values of C_{export} were 379 ± 38 and 78 ± 8 g C m^{-2} yr^{-1}, respectively, assuming an uncertainty of ±10%.

The CO_2 equivalent flux of each non-CO_2 GHG was obtained by multiplying the cumulative flux by the respective value of the mass-based global warming potential (GWP). The GWPs of N_2O and CH_4 (i.e., GWP_{N_2O} and GWP_{CH_4}) for a 100-year time scale are 273 and 27 (Forster et al., 2021), respectively. The annual GHG balance of each crop was obtained by summing the CO_2 equivalent fluxes of the GHGs over the year as follows (Lee et al., 2017):

$$F_{CO_2}e = m_{CO_2}\mathrm{NEE} + \mathrm{GWP}_{CH_4} m_{CH_4} F_{CH_4} + \mathrm{GWP}_{N_2O} m_{N_2O} F_{N_2O} \tag{4}$$

where $F_{CO_2}e$ is the sum of the CO_2 equivalent mass fluxes of CO_2, CH_4, and N_2O (i.e., the balance of GHGs). F_{CO_2} (i.e., ~NEE), F_{CH_4} and F_{N_2O} are the study-period total molar fluxes, and m_{CO_2}, m_{CH_4}, and m_{N_2O} are the molar masses of the respective GHGs.

Uncertainties in CO_2, CH_4, and N_2O fluxes were determined following Pow et al. (2020) and included respective values of the measurement error, gap-filling error, and systematic error in the selection of the u_* threshold.

2.4. Flux Footprint Analysis

2.4.1. Flux Footprint Model

To determine the source area of fluxes, the Flux Footprint Prediction model (FFP) proposed by Kljun et al. (2015) was used. Indicated by the annual flux footprint climatology (Figure S2 in Supporting Information S1), the 80% contour line, the source area determined by the model to account for 80% of the measured flux, was within the west and east crop fields. The EC-measured fluxes at this site are the result of surface fluxes from two parts of the field: the crop area and the edge area. Although the edge area is small compared to the crop area, its proximity to the EC mast can greatly affect the EC fluxes. Thus FFP was further used to correct for this edge effect and to obtain the surface fluxes from the crop area of interest. For each half hour, we calculated the flux footprint over the whole domain around the tower at 1-m resolution. The EC flux over the integrated area can be expressed as follows (Kljun et al., 2015):

$$F_{\mathrm{EC}} = \int Q(x,y) f(x,y) dx dy \tag{5}$$

where F_{EC} is the flux measured by the EC system, $Q(x,y)$ is the surface flux at location (x,y), $f(x,y)$ is the footprint contribution to the EC flux at location (x,y) and $dxdy$ is the unit size of the source area, which is 1 m^2 in this case.

When the surface fluxes from each landscape component (the crop and edge areas) are available, the fluxes measured by EC can be expressed as follows:

$$F_{\mathrm{EC}} = \int_c Q_c(x,y) f_c(x,y) dx dy + \int_e Q_e(x,y) f_e(x,y) dx dy \tag{6}$$

where the subscript c denotes the crop area and e denotes the edge area adjacent to the crop area. To simplify the computation of the footprint contributions, Q_c and Q_e were assumed to be uniform within the crop and edge areas, respectively, since both landscape components were relatively homogeneous. Therefore, F_{EC} can be expressed as follows:

$$F_{\mathrm{EC}} = Q_c \sum f_c(x,y) + Q_e \sum f_e(x,y) \tag{7}$$

where $\sum f_c(x,y)$ and $\sum f_e(x,y)$ are the summations of the footprint contributions over the crop and edge areas, respectively, according to the actual sizes of these two landscape components. The two summations will now be referred to as f_c and f_e, respectively. They were calculated for each half hour using an online Matlab program created by N. Kljun (Kljun et al., 2015).

2.4.2. Flux Footprint Corrections of EC Fluxes

2.4.2.1. N_2O

Using Equation 8, the N_2O flux measured by the EC system (F_{N_2O}) from the crop and the edge areas can be expressed as follows:

$$F_{N_2O} = Q_{c\_N_2O} f_c + Q_{e\_N_2O} f_e \tag{8}$$

where $Q_{c\_N_2O}$ and $Q_{e\_N_2O}$ are the surface fluxes of N_2O in the crop and the edge areas, respectively. $Q_{e\_N_2O}$ was obtained using nonsteady state flux chamber measurements during daytime because no appreciable diurnal variations of F_{N_2O} were observed. An expression for $Q_{c\_N_2O}$ can be obtained by rearranging Equation 8 as follows:

$$Q_{c\_N_2O} = \left(F_{N_2O} - Q_{e\_N_2O} f_e\right) / f_c \tag{9}$$

2.4.2.2. CO_2

The entire data analysis procedure for the CO_2 flux is shown as a flowchart in Figure S3 of Supporting Information S1. First, the net ecosystem exchange measured by the EC system (i.e., NEE) can be expressed as follows:

$$\mathrm{NEE} = Q_{c\_nee} f_c + Q_{e\_nee} f_e \tag{10}$$

where Q_{c_nee} and Q_{e_nee} are the values of NEE of the crop and the edge areas, respectively. An equation similar to Equation 10 can be written for R_e (= NEE measured by the EC system during nighttime) as follows:

$$R_e = Q_{c\_re} f_c + Q_{e\_re} f_e \tag{11}$$

where Q_{c_re} and Q_{e_re} are the values of R_e of the crop and the edge areas, respectively. The values of f_c and f_e remain the same as those in Equation 10 for each half hour. Subtracting Equation 10 from Equation 11 results in the corresponding equation for the EC-measured GPP as follows:

$$\mathrm{GPP} = Q_{c\_gpp} f_c + Q_{e\_gpp} f_e \tag{12}$$

where $Q_{c\_gpp} = Q_{c\_re} - Q_{c\_nee}$ and $Q_{e\_gpp} = Q_{e\_re} - Q_{e\_nee}$ which are the GPP values for the crop and the edge areas, respectively. Rearranging Equation 12 provides an expression for Q_{c_gpp} as follows:

$$Q_{c\_gpp} = \mathrm{GPP}/(f_c + k f_e) \tag{13}$$

where k is the ratio of Q_{e_gpp} to Q_{c_gpp}. Based on typical GPP (Q_{c_gpp}) values of a grass crop reported in the literature (e.g., Sheehy & Peacock, 1975) and our estimated $Q_{c_{gpp}}$ (Appendix A2), we considered three values of k (0.8, 1.0, and 1.2) in this analysis. A short experiment aimed at roughly estimating the sink strength of the grass by using tarpaulins to cover grass along the edge just north-west of the flux tower conducted in May 2019 confirmed this range of k values (see Appendix A2).

Nighttime Q_{e_re} was obtained using the logarithmic relationship ($\ln Q_{e\_re} = A + BT_s$) between daytime Q_{e_re} measured using the chamber and T_s. Nighttime Q_{c_re} was calculated using Equation 11 for each half hour. Then Q_{c_re} during the daytime was obtained by developing a relationship between Q_{c_re} and corresponding T_s during the nighttime but using daytime T_s. Therefore, daytime R_e was calculated using Equation 11, and with NEE directly measured by the EC system, GPP was obtained using Equation 1. Then Q_{c_gpp} was obtained using Equation 13. Finally, Q_{c_nee} was determined using:

$$Q_{c\_nee} = Q_{c\_re} - Q_{c\_gpp} \tag{14}$$

2.4.2.3. CH_4

Chamber-measured CH_4 fluxes from the crop and the edge areas were generally negligible with very small emissions occasionally occurring possibly from the ditch. Therefore, no flux footprint correction was applied to the EC-measured CH_4 fluxes.

3. Results and Discussion

3.1. Meteorological and Soil Variables

Meteorological variables during the study period (May 2018 to October 2019) are shown in Figure 4. During this period, the annual mean T_a was 10.8°C with the monthly mean T_a ranging from 1.0°C (February 2019) to 18.2°C (August 2018). The site received an annual (1 August 2018–31 July 2019) P of 976 mm, of which approximately 80% occurred between 1 September 2018 and 28 February 2019. The largest monthly P was observed in December 2018, with a total of 201 mm. Growing season (1 May to 30 September) total P was less in 2018 (153.9 mm) than in 2019 (186.6 mm). While values of monthly and annual mean T_a at the site were very close to the long-term mean values at YVR, annual P at the site was lower than the long-term mean at YVR, with the growing season (May to August) of 2019 being drier and December 2018 appreciably wetter. Average daytime vapor pressure deficit (D_{day}) was generally <0.5 kPa during the non-growing season but slightly exceeded 1 kPa during the growing season.

Daily average T_s at the 5-cm depth followed the same pattern as T_a, with a larger difference between the two during the summer months (Figure 4a). Daily mean T_s was always >0°C while daily mean T_a dropped slightly below 0°C during early February in 2019. Soil volumetric water content measured at the 5-cm depth (θ_s) increased in September 2018 following heavy precipitation and reached the maximum (approximately 0.50 $m^3\ m^{-3}$, near saturation) in January 2019. A steep drop in θ_s occurred in February 2019, coinciding with the lowest daily mean T_a which was −5°C. Other than that, θ_s remained high throughout the spring and then gradually declined to approximately 0.25 $m^3\ m^{-3}$ during the growing season (Figure 4e). This was much higher than the permanent wilting point (−1.5 MPa matric potential) value of 0.15 $m^3\ m^{-3}$ for this soil.

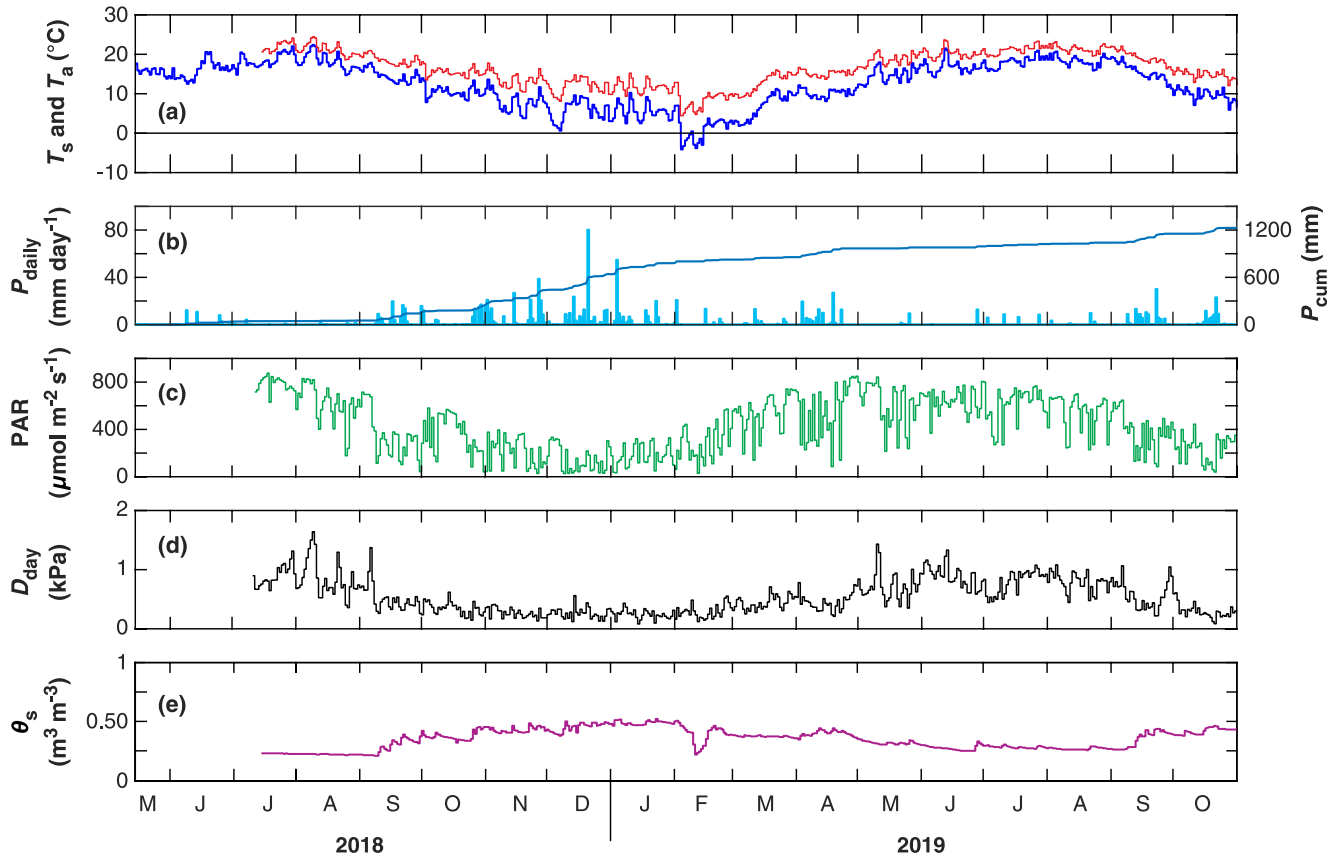

Figure 4. Climate variables at the site during the study period. (a) Daily average soil temperature at the 5-cm depth (T_s) (red solid line) and daily average air temperature (T_a) (blue solid line) (b) 1-day precipitation (P_{Daily}) and cumulative precipitation (P_{Cum}). (c) Daytime average photosynthetically active radiation (PAR). (d) Daily average daytime vapor pressure deficit (D_{day}). (e) Daily average soil volumetric water content at the 5-cm depth (θ_s). Daytime was determined by solar irradiance >0 W m^{-2}. The data of from mid-May to mid-July were gap filled using data from Vancouver International Airport (12 km north of the site).

3.2. N_2O Fluxes

3.2.1. Comparison of EC-Measured and Flux-Footprint-Corrected N_2O Fluxes

There was a strong linear relationship between half-hourly EC-measured fluxes (F_{N_2O}) and footprint-corrected fluxes ($Q_{c\_N_2O}$) with the latter being 40% and 51% higher than the former for the west and east fields, respectively (Figure 5). For the combined data for both fields, half-hourly $Q_{c\_N_2O}$ was 43% higher than F_{N_2O} (R^2 of 0.97, RMSE = 0.23 nmol m^{-2} s^{-1}). A strong linear relationship was also found between monthly $Q_{c\_N_2O}$ and F_{N_2O} (R^2 = 0.95; results not shown). This suggests that it would be possible to apply a conversion coefficient to the fluxes measured by the EC system to correct for the effect of the edge area. This coefficient would likely be site specific but applicable with a proportional footprint contribution from the edge area being relatively constant. EC-measured total F_{N_2O} values for the potato growing season (west and east fields as a whole), the potato non-growing season, the pea growing season (east field only), and the pea non-growing season were 0.37, 0.59, 0.07, and 0.67 g N_2O-N m^{-2}, respectively. After applying footprint correction, we found the respective $Q_{c\_N_2O}$ totals were 0.51, 0.86, 0.11, and 0.98 g N_2O-N m^{-2}, respectively (Table S1 in Supporting Information S1).

Measured annual N_2O emissions from potato fields have been found to be about 2.0 and 0.5 kg N_2O-N ha^{-1} in southern Germany (mean temperature at 7.4°C and mean annual precipitation at 803 mm) and northern China (mean temperature at 3.2°C and mean annual precipitation at 343 mm), respectively (Flessa et al., 2002; Wang et al., 2017). These values are very low compared to ours (5.1 kg N_2O-N ha^{-1}). The potential reason could be the higher temperature and precipitation at our site. A pea field in Switzerland with a mean annual temperature of 8.8°C and mean annual precipitation of 1,088 mm emitted 1.4 kg N_2O-N ha^{-1} over the growing season in 2019 (Maier et al., 2022), which was close to our results (1.1 kg N_2O-N ha^{-1}). Pattey et al. (2008) also measured similar N_2O emissions (1.7 kg N_2O-N ha^{-1}) in eastern Canada even though their field experienced lower temperature.

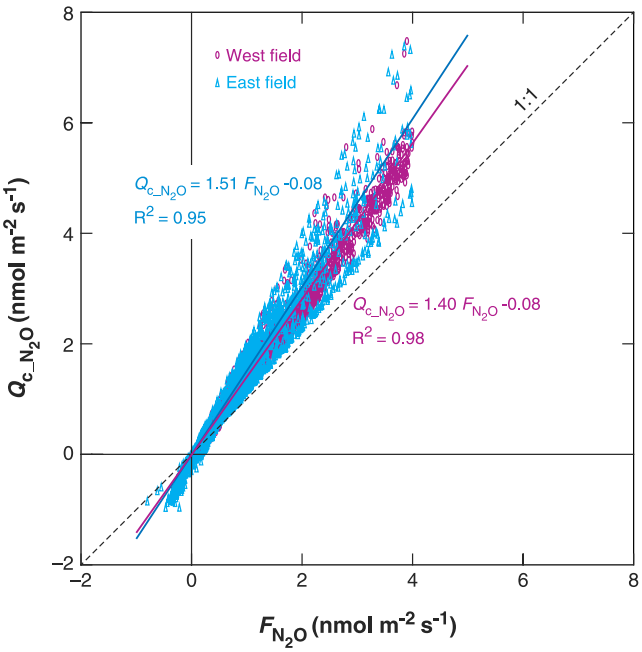

Figure 5. Linear relationships between half-hourly N_2O fluxes corrected for the edge effect ($Q_{c\_N_2O}$) and those measured by EC (F_{N_2O}) for the west (purple circles) and east (blue triangles) fields during the entire study period. The purple and blue lines are the linear regression lines for the west and east fields, respectively, and the dashed line is the 1:1 line. Coefficients and model parameters for the linear relationships are also shown.

Much lower N_2O emissions over three consecutive pea cropping seasons (0.03–0.9 kg N_2O-N ha^{-1}) were observed in France (Jeuffroy et al., 2013). It is noteworthy that except for Maier et al. (2022) and Pattey et al. (2008), the other studies used the flux chamber technique to quantify N_2O emissions, and that lower emissions could likely be due to missing large peaks of highly episodic N_2O emissions with much lower chamber measurement frequency (Merbold et al., 2021).

We found that the chamber-measured N_2O fluxes from the edge area were between 0 and 1 nmol m^{-2} s^{-1}, similar to the background (i.e., before N fertilizer application) F_{N_2O} measured by the EC system. However, while the edge area was a weak source, much higher EC-measured N_2O flux pulses (>1.5 nmol m^{-2} s^{-1}) were constantly observed during the study period.

3.2.2. Temporal Variation of N_2O Flux

The potato field (east and west) and pea field (east) were N_2O sources during the entire study period (Figure 6). After the fertilization in mid-May 2018, $Q_{c\_N_2O}$ of the potato field peaked at approximately 3.8 nmol m^{-2} s^{-1} likely due to the increased NO_3^- in the soil enhancing the denitrification process (Gillam et al., 2008). Relatively high soil temperatures during the summer months of June and July favored soil microbial activity, resulting in higher $Q_{c\_N_2O}$ which remained elevated for about 8 weeks. Then it declined to less than 0.2 nmol m^{-2} s^{-1} for the rest of the potato growing season, likely due to nitrogen uptake by the crop. After tuber harvest (18 September 2018), N_2O production was stimulated by frequent rainfall events and multiple $Q_{c\_N_2O}$ pulses were observed with the highest value being approximately 4.2 nmol m^{-2} s^{-1} near the end of September 2018. It has been found that precipitation can greatly affect N_2O emissions from agricultural soils (Nielsen & Ball, 2015; Pihlatie et al., 2004; Saarnio et al., 2013; Schaufler et al., 2010). By using EC measurements, Huang et al. (2014) found that N_2O emissions from a corn field in Tennessee USA responded quickly to rainfall events and increased within 30 min. This was also observed on a silage farm in Australia (Phillips et al., 2013). In addition, the presence of organic matter from potato crop residues can promote sufficient heterotrophic respiration to create or enlarge anaerobic microsites in which denitrification can take place (Smith et al., 1997; Tiedje et al., 1984). Surprisingly, similar N_2O emission pulses after fertilizer application in the pea field did not occur,

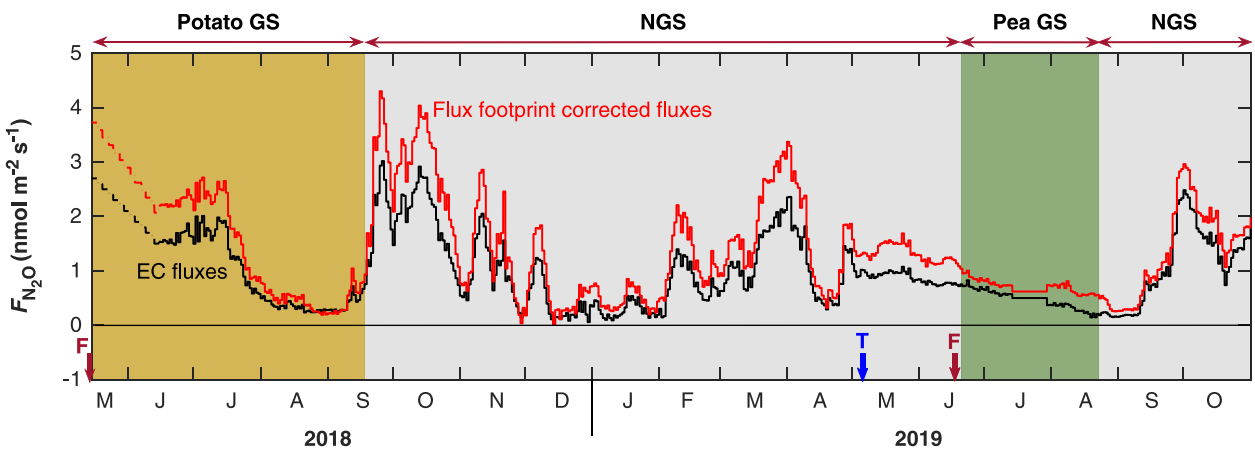

Figure 6. Daily average N_2O fluxes measured by EC (F_{N_2O}; black solid line) and N_2O fluxes corrected for the edge effect ($Q_{c\_N_2O}$; red solid line) using the flux footprint analysis and the chamber measurements made in the edge area during the study period. Refer to Figure 2 for the definition of the different periods. The red and blue vertical arrows indicate fertilizer (*F*) application and tillage (*T*) events, respectively. The red dashed line ($Q_{c\_N_2O}$) from mid-May to mid-June 2018 was obtained by linear interpolation of chamber measurements made in the crop. The black dashed line (F_{N_2O}) from mid-May to mid-June 2018 was obtained using a fixed coefficient, $Q_{c\_N_2O}/F_{N_2O}$ = 1.39 obtained from measurements made during the potato GS (20 June 2018–18 September 2018). The laser spectrometer malfunctioned from 16–28 July 2019 but chamber measurements confirmed no change in N_2O emissions during this period.

possibly due to several factors such as the lower fertilization rate compared to that for potatoes, faster pea crop growth and hence nitrogen uptake, and environmental conditions or the result of interactions among these factors. However, a similar $Q_{c\_N_2O}$ response to rainfall events occurred in late September and October 2019, with $Q_{c\_N_2O}$ reaching 3.0 nmol m^{-2} s^{-1}. The highest monthly total $Q_{c\_N_2O}$ (0.21 g N_2O-N m^{-2} $month^{-1}$) was observed in October 2018 (Table S1 in Supporting Information S1). Based on the footprint-corrected fluxes, the growing season N_2O emissions total for the pea crop was only 22% of that for the potato crop (Table S1 in Supporting Information S1). Large emissions during the non-growing season accounted for approximately 61% and 90% of the annual emissions for the potato year and the pea year, respectively. This emphasizes the importance of mitigating the N_2O emissions especially during the non-growing season in a region where the weather during that period is characterized by heavy precipitation. According to Drever et al. (2021), it is critical to decrease GHG emissions from agricultural soils by growing cover crops during non-growing season. Cover cropping has been found to successfully reduce GHG emissions with no negative effects on cash crop yields in different crop fields (Bavin et al., 2009; Behnke & Villamil, 2019). By using data from five contrasting sites, Tribouillois et al. (2018) predicted that cover crops have the potential to lower the GHG balance by 315 kg CO_2e ha^{-1} $year^{-1}$ over 45 years compared to that of bare soil in France. Globally, cover crops, through their effect on GHG fluxes, are estimated to mitigate warming by between 1.00 and 2.06 Mg CO_2e ha^{-1} $year^{-1}$ (Abdalla et al., 2019; Kaye & Quemada, 2017). It is interesting to note that daily average $Q_{c\_N_2O}$ values were higher than those from a nearby blueberry field (~1 km away) fertilized with a similar amount of fertilizer as that for the potato field (~110 kg N ha^{-1}). Although blueberry is a perennial crop, we suspect that this is likely due to the fertilizer being applied to the blueberry field 4 times during the growing season, resulting in higher N use efficiency and thus lower N_2O emissions (Pow et al., 2020). However, the relationship between N fertilization (i.e., different type and mixed composition) and N_2O fluxes can be complex (Ma et al., 2022). It has been found that N_2O emissions increased substantially when N inputs exceeded crop needs (Shcherbak et al., 2014). Replacing 25% of mineral fertilizer with organic manure can greatly decrease N_2O emissions (Lv et al., 2020). Chizen et al. (2022) concluded that lower N fertilizer rates (<100 kg N ha^{-1}), especially in fields with degraded soils, can lower N_2O emissions from potato production in British Columbia. Recently, Thilakarathna et al. (2023) evaluated different nitrogen management practices and found application of nitrification inhibitors has substantial potential to reduce N_2O emissions in Canada.

3.3. CH_4 Flux

Over the entire study period, F_{CH_4} values were generally very small, with evidence of both production and consumption of small amounts of CH_4 (Figure S4 in Supporting Information S1). Overall the potato and pea fields were very weak sources of CH_4. Daily average F_{CH_4} was between 0 and 5 nmol m^{-2} s^{-1} for most of the observation period while some relatively high values larger than 5 nmol m^{-2} s^{-1} were occasionally observed. The possible reason could be that decomposition mainly happened in aerobic conditions that would only allow small CH_4 fluxes (Saunois et al., 2020). Low CH_4 emissions were also measured in a pea-maize field in Switzerland (Maier et al., 2022). Some high F_{CH_4} values likely resulted from the CH_4 emissions from the ditch, similar to those observed by Needelman et al. (2007) and Peacock et al. (2021). However, the magnitude of F_{CH_4} from the ditch could not be determined without careful and regular chamber measurements taken above the water surface of the ditch. In addition, the bare soil after the crop harvest experienced poorly drained periods of time after frequent rainfall events, which could also contribute to CH_4 emissions due to anaerobic soil conditions favoring CH_4 production (Conrad, 2020; Ehhalt & Schmidt, 1978). However, these emissions are difficult to partition from the fluxes measured by the EC system without confirmed surface fluxes from the ditch. CH_4 totals for the potato growing season (west and east fields as a whole), the potato non-growing season, the pea growing season (east field only), and the pea non-growing season were 0.46, 0.59, 0.40, and 0.71 g CH_4-C m^{-2}, respectively (Table S2 in Supporting Information S1).

3.4. CO_2 Flux Components

3.4.1. Comparison of EC-Measured and Flux-Footprint-Corrected CO_2 Flux Components

Flux footprint corrections for the CO_2 flux components were, in general, small. The largest corrections were to R_e (Figure 7) which was due to the differences between soil respiration of the edge and R_e of the crop. It is important to note that we used soil respiration from chamber measurements to approximate R_e of the edge area. It is likely that this may have resulted in an underestimation of Q_{e_re} by 20%–30% (Lohila et al., 2003). During the

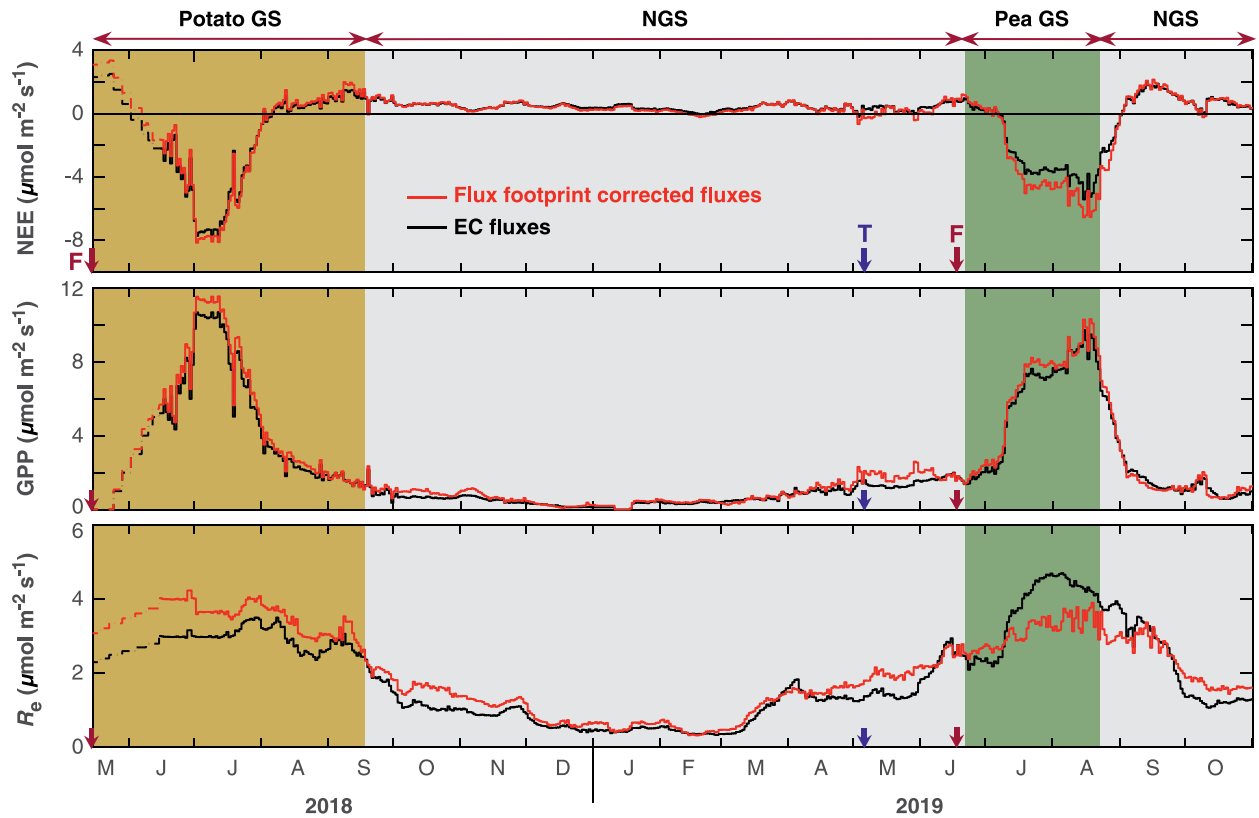

Figure 7. Temporal variations in EC-measured (black lines) flux-footprint-corrected for $k = 1$ (red lines) of daily NEE, GPP and R_e, respectively. Refer to Figure 2 for the definition of the different periods. The red and blue vertical arrows indicate fertilizer application events (F) and tillage events (T), respectively. The dashed lines from mid-May to mid-June 2018 was obtained based on chamber measurements (R_e) made in the crop and an estimation from the progression behavior of GPP at the beginning of the crop growing season.

potato growing season, footprint-corrected R_e was about 15% higher than uncorrected R_e (or ~0.4 μmol m^{-2} s^{-1} higher). It remained higher during the non-growing season between the potato and the pea crop growing seasons. Footprint-corrected GPP using $k = 1$ was very similar to EC-derived GPP thereby supporting our hypothesis that the photosynthesis of the grass component of the edge area was quite similar to that of the crop. Finally, as a result of the edge effect on R_e, footprint-corrected NEE deviated slightly from EC measurements particularly during the latter half of the pea growing season when the magnitude of EC-measured NEE was underestimated by on average 0.7 μmol m^{-2} s^{-1}.

GPP increased gradually after each crop emerged and developed, reaching the highest daily mean values ($k = 1$) of 11 and 10 μmol m^{-2} s^{-1} during the potato and pea growing seasons, respectively. After the first half of the potato growing season, potato growth transitioned from vegetative growth to tuber bulking, and then to maturation, and GPP decreased until harvest as the vines senesced and lost leaves. Unlike the potato crop, the pea vine remained green until harvest, so the steep drop of GPP occurred outside the defined pea growing season. The highest monthly GPP was observed in July 2018 (302 g C m^{-2} $month^{-1}$) for the potato crop, and in August 2019 (250 g C m^{-2} $month^{-1}$) for the pea crop (Table S3 in Supporting Information S1, $k = 1$). In contrast to other studies (Gilmanov et al., 2013; Patel et al., 2021), we did not observe a decrease in GPP under high VPD conditions, which can decrease stomatal conductance and limit crop photosynthetic rate (Song et al., 2022). Potential reasons are that the study crop fields did not experience very high VPD (peak half-hourly value being about 1.5 kPa) and the soil moisture content maintained at a level much higher than the wilting point value.

Compared to the temporal patterns of GPP, crop-specific seasonal differences in R_e were less pronounced. Maximum R_e was very similar (~4 μmol m^{-2} s^{-1}) in the growing season of the two crops. After potato harvest, R_e declined slowly, likely due to slower decomposition of the fresh residues left on the field at lower soil temperatures in September. Subsequently, non-growing season R_e remained relatively low at approximately 0.5 μmol m^{-2} s^{-1}

Table 1
Annual Ecosystem Respiration (R_e), Gross Primary Production (GPP), Net Ecosystem Exchange (NEE) Measured by Eddy Covariance (EC), Carbon Removal From Crop Harvest, Carbon Addition From Seeding, and Net Ecosystem Carbon Balance (NECB) for the Potato and Pea Crops Without Flux Footprint Correction (EC-Measured) and With Flux Footprint Correction Using k = 1 ($k = Q_{e\_gpp}/Q_{c\_gpp}$)

	Potatoes		Peas	
	EC-measured	$k = 1$	EC-measured	$k = 1$
R_e (g C m^{-2} yr^{-1})	601 ± 100	736 ± 122	642 ± 106	652 ± 108
GPP (g C m^{-2} yr^{-1})	671 ± 111	793 ± 131	672 ± 111	749 ± 124
NEE (g C m^{-2} yr^{-1})	−70 ± 11	−57 ± 9	−30 ± 5	−97 ± 16
Carbon removal from crop harvest (g C m^{-2} yr^{-1})	379 ± 38	379 ± 38	78 ± 8	78 ± 8
Carbon addition from seeding (g C m^{-2} yr^{-1})	38 ± 8	38 ± 8	11 ± 2	11 ± 2
NECB (g C m^{-2} yr^{-1})	−271 ± 57	−284 ± 55	−37 ± 15	30 ± 26

Note. The potato year was from 15 May 2018 to 14 May 2019 and the pea year was from 1 October 2018 to 30 September 2019.

throughout the winter and increased to 2 μmol m^{-2} s^{-1} when soil temperature started to increase prior to the pea growing season. The difference between growing season and non-growing season R_e is due to both the difference in soil temperature as well as the absence of autotrophic respiration (R_a) during the non-growing season as R_a can account for 60%–90% of total R_e during the growing season (Suleau et al., 2011). Non-growing season R_e which is mainly heterotrophic respiration was 50% and 62% of annual R_e during the potato and pea years, respectively, partly as a result of the period without active vegetation cover being very long (8 and 10 months for the potatoes and peas, respectively). Unlike the pea growing season, average footprint-corrected R_e values were higher during the potato growing season (Table S4 in Supporting Information S1), likely due to higher autotrophic and heterotrophic respiration, which can be attributed to higher biomass and intensive pre-planting tillage, respectively.

Overall, the ecosystem-stored C from June to July 2018 for the potato crop and from July to August 2019 for the pea crop, with GPP being higher than R_e. Similar to the results reported by Ceschia et al. (2010), we found that the length of time when there was photosynthetically active vegetation cover closely corresponded to the number of days that C was stored by the ecosystem (i.e., NEE <0), which were 56 and 64 days, for potato and pea crops, respectively. The growing season footprint-corrected NEE values for $k = 1$ were −144 and −208 g C m^{-2} for the potato and pea crops, respectively, while the non-growing season values were 87 and 111 g C m^{-2}, respectively (obtained from the Q_{c_gpp} and Q_{c_er} values in Tables S3 and S4 in Supporting Information S1, respectively). The corresponding EC-measured values are shown in Table S5 of Supporting Information S1 while Table S6 in Supporting Information S1 shows annual GPP, R_e, and NEE values for the two crops for different k values.

3.4.2. Annual Net Ecosystem Exchange and Net Ecosystem Carbon Balance

For both the potato and the pea fields, annual CO_2 uptake exceeded CO_2 release, resulting in a net uptake of 57 ± 9 g C m^{-2} yr^{-1} (i.e., NEE = −57 g C m^{-2} yr^{-1} ranging from −101 to −21 g C m^{-2} yr^{-1} when k varied from 0.8 to 1.2, respectively) and 97 ± 16 g C m^{-2} yr^{-1} (i.e., NEE = −97 g C m^{-2} yr^{-1} ranging from −122 to −76 g C m^{-2} yr^{-1} when k varied from 0.8 to 1.2, respectively) for the potato and pea fields, respectively (Table 1 and Table S6 in Supporting Information S1). The corresponding uncorrected EC values for the potato and pea fields were −70 ± 11 and −30 ± 5 g C m^{-2} yr^{-1}, respectively (Table S5 in Supporting Information S1). The annual EC and footprint-corrected values were similar for potatoes but much different for peas. This is because the footprint-corrected values of NEE during the pea growing season were approximately 1 μmol m^{-2} s^{-1} more negative than the EC values. Anthoni et al. (2004) found that the annual NEE for a potato crop in Germany with reduced tillage was −34 g C m^{-2} yr^{-1} (ranging from −49 to 29 g C m^{-2} yr^{-1}), which is comparable to that for the potato crop in this study. Gilmanov et al. (2014) reported that year-round annual legume crops at 17 flux tower sites in North America and three sites in Europe demonstrated a wide range of NEP (i.e., -NEE) values, with an average of −90 g C m^{-2} yr^{-1} (ranging from C sinks of 207 g C m^{-2} yr^{-1} to C sources of 573 g C m^{-2} yr^{-1}). The average value of annual NEP in their study indicated overall tendency for legume crops to be C sources, while the pea crop in this study was a moderate C sink.

The annual footprint-corrected GPP for the potato crop with a 4-month growing season (793 ± 131 g C m^{-2} yr^{-1}, ranging from 837 to 757 g C m^{-2} yr^{-1} for $k = 0.8$ and 1.2, respectively) was similar to that for the pea crop with a shorter 2-month growing season (749 ± 124 g C m^{-2} yr^{-1}, ranging from 775 to 728 g C m^{-2} yr^{-1} for $k = 0.8$ and

Table 2
CO_2, N_2O, and CH_4 Expressed in CO_2 Equivalents (CO_2e) and the Greenhouse Gas (GHG) Balances of Greenhouse Gases (Positive Values Indicate Loss to the Atmosphere) for the Potato and Pea Years (g CO_2e m^{-2} yr^{-1}) Without Flux Footprint Correction (EC-Measured) and With Flux Footprint Correction With k (i.e., Q_{e_gpp}/Q_{c_gpp}) = 1

Crop		CO_2	N_2O—CO_2e	CH_4—CO_2e	GHG balance
Potatoes	EC-measured	−257 ± 43	412 ± 22	38 ± 21	193 ± 86
	$k = 1$	−209 ± 35	588 ± 32	38 ± 21	417 ± 88
Peas	EC-measured	−110 ± 18	317 ± 17	40 ± 22	247 ± 57
	$k = 1$	−356 ± 59	468 ± 25	40 ± 22	152 ± 106

Note. The potato year was from 15 May 2018 to 14 May 2019 and the pea year was from 1 October 2018 to 30 September 2019.

1.2, respectively), as a result of the differences in the intensity and pattern of photosynthetic assimilation between the two crops (Table 1 and Table S6 in Supporting Information S1). The corresponding EC values of GPP for the potato and pea fields were 671 ± 111 and 672 ± 111 g C m^{-2} yr^{-1}, respectively. The annual value of the footprint-corrected R_e for the pea crop (652 ± 108 g C m^{-2} yr^{-1}) was much less than that for the potato crop (736 ± 122 g C m^{-2} yr^{-1}). Overall, values in Table 1 suggest that the potato and pea fields in this study were weak C sinks with the pea field being slightly stronger.

To obtain the NECB, NEE was combined with estimates of C_{export} and C_{import} (Equation 3). Based on the NECB values, the potato field shifted from being a weak C sink to being a moderately strong C source (−284 ± 55 g C m^{-2} yr^{-1}), while the pea field shifted from being a weak C sink to being a very weak C sink (30 ± 26 g C m^{-2} yr^{-1}) (Table 1). This was the result of the large C export from the potato field and small C export from the pea field. Similar results that a large proportion of the C accumulation is exported from the site has been reported and discussed widely for cropland ecosystems (Ceschia et al., 2010; Ciais et al., 2001; Gilmanov et al., 2010). Ceschia et al. (2010) reported an average NECB of −138 ± 239 g C m^{-2} yr^{-1} for European croplands representing an annual loss of 2.6% of soil organic carbon. Their corresponding value of NEE was −284 ± 228 g C m^{-2} yr^{-1} pointing to the importance of C exports in the NECB. As pointed out by Gilmanov et al. (2010), the ability of managed agroecosystems to serve as sinks of CO_2 from the atmosphere depends on the ultimate fate of the harvested biomass. Wiesner et al. (2022) observed that an intermediate wheatgrass monoculture accumulated more C with an NECB of 306 ± 88 g C m^{-2} than a biculture with red clover being C neutral (NECB = 7 g ± 131 g C m^{-2}) on a dairy farm in Wisconsin, USA. Kim et al. (2022) found that the two perennial crop fields in the Canadian prairies had NECB values of −60 (weak C source) and 448 (strong C sink) g C m^{-2}, respectively. However, another two annual crop fields were both C sources (−263 and −336 g C m^{-2}, respectively). They suggested the perennial crop enhanced the atmospheric C sink compared to the annual crop but also noted their assessment did not account for non-CO_2 C (e.g., CH_4) emissions.

When estimating the NECB, a large uncertainty associated with calculating C input and C output is often expected given that the information provided by farmers may be approximate. Given that NEE and C export have the greatest impact on the annual C balance of croplands (Ceschia et al., 2010), the importance of more accurate C export estimates should be stressed in future studies.

3.5. Annual GHG Balances of the Potato and Pea Crops

3.5.1. GHG Balances

Summation of footprint-corrected CO_2e values of the three GHGs yielded ($k = 1$) a net GHG balance of 417 ± 88 g CO_2e m^{-2} yr^{-1} (ranging from 256 to 574 g CO_2e m^{-2} yr^{-1} for $k = 0.8$ and 1.2, respectively) for the potato field, and 152 ± 106 g CO_2e m^{-2} yr^{-1} (ranging from 61 to 251 g CO_2e m^{-2} yr^{-1} for $k = 0.8$ and 1.2, respectively), for the pea field (Table 2 and Table S7 in Supporting Information S1), indicating that both fields acted as net sources of GHGs on an annual basis. The corresponding EC values of annual GHG balances for the potato and pea fields were 193 ± 86 and 248 ± 57 g CO_2e m^{-2} yr^{-1}, respectively. The former value was much smaller than the footprint-corrected value ($k = 1$) mainly because the footprint-corrected N_2O CO_2e was about 200 g CO_2e m^{-2} yr^{-1} larger than the EC-measured N_2O CO_2e value (Figure 6 and Table S7 in Supporting Information S1). In the case of the pea field, the EC-measured GHG balance was larger than the footprint-corrected value mainly because footprint correction resulted in an appreciably more negative NEE (i.e., −356 ± 59 g CO_2 $m^{-2}y^{-1}$) as mentioned in Section 3.4.2. Recently, Maier et al. (2022) used a similar setup (i.e., sonic anemometer with a laser spectrometer) to measure GHG fluxes from a pea field in Switzerland, and found the GHG balance for the pea crop to be about −450 g CO_2e m^{-2} over 55 days. This value is smaller than our footprint-corrected GHG balance for the pea crop over the growing season (i.e., about −700 g CO_2e m^{-2}) considering our pea growing season was 9 days more than theirs and their pea crop was not fertilized.

Similar patterns of the contribution of different GHGs to the annual GHG balances were observed for both crop fields. Uptake of CO_2 was offset by relatively large N_2O emissions (588 ± 32 and 468 ± 25 g N_2O-CO_2e m^{-2} yr^{-1}, $k = 1$, for the potato and pea crops, respectively), with the N_2O emissions strongly contributing to

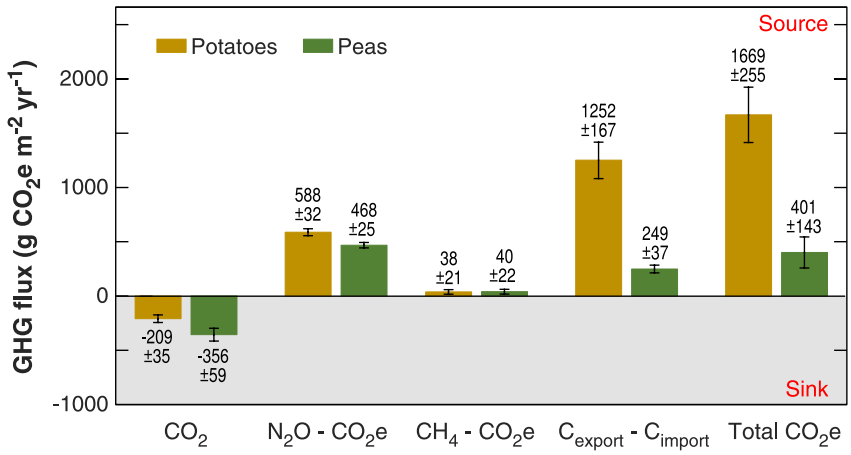

Figure 8. The greenhouse gas (GHG) balances (g CO_2e m^{-2} yr^{-1}) of CO_2, N_2O, and CH_4 with the difference between export of potato tubers and peas (C_{export}) and import of seed potatoes and pea seeds (C_{import}) from the field for the potato and pea years using flux footprint correction with $k = 1$ and accounting for the global warming potentials.

global warming. The substantial contribution of N_2O emissions (i.e., up to 66%) to the GHG balance was also observed from a fertilized sugar beet field in Belgium (Lognoul et al., 2019). This again highlights how critical it is to include N_2O emissions when assessing the GHG budget from a fertilized crop. CH_4 accounted for a small proportion of the annual GHG balances (10% and 25%, $k = 1$, for the potato and pea fields, respectively) (Table 2). Caution should be taken when comparing these two crop years as they share a common non-growing season, as a considerable proportion (63% and 90% for the potato and pea crops, respectively) of N_2O emissions occurred outside the growing season. It is possible that the time period following pea harvest may have exhibited a different pattern of N_2O emissions under different climate conditions from that of the common non-growing season in this study. Under similar climate conditions (P, T_s, and θ_s; see Figure 4) in the months of September and October in both 2018 and 2019, a lower rate of N_2O emissions following pea harvest likely resulted from a lower N application rate to the pea crop. Furthermore, after harvest the standing pea crop was sequestering CO_2 (see Figure 7) so that (a) some soil N was likely still being taken up by the crop and (b) the pea biomass was not yet in a state of active decomposition as was the case following potato harvest thereby minimizing N_2O emissions during the beginning of the pea NGS. In the case of CO_2, given that R_e was constantly low and did not exhibit an obvious temporal variation responding to changing weather during the winter, it likely did not contribute much to the non-growing season R_e in the pea year (Figure 7). However, it should be noted that the period (approximately 2 weeks) following the preparation of the potato field for planting was not included in the potato year in our study. It is recognized that tillage used in field preparation, which is always intensive for potatoes in this region, might have resulted in a notable increase in R_e and consequently a more positive NEE for the potato year. For example, Abdalla et al. (2016) synthesized 46 peer-reviewed publications and found tilled soils significantly emitted 21% more CO_2 on average than untilled soils. A wheat-maize rotation crop field in the North China Plain has been found to emit more CO_2 under conventional tillage (65 g CO_2-C m^{-2} y^{-1}) than with no tillage (39 g CO_2-C m^{-2} y^{-1}) (Wu et al., 2017). Similarly, deep tillage has been observed to increase total CO_2 emissions by between 4.9% and 37.7% in another wheat field in North China (Gong et al., 2022).

3.5.2. Accounting for C Imports and Exports in GHG Balances

Figure 8 summarizes the contributions of the GHG fluxes and C imports and exports to the annual GHG balances for the two crops. Estimation of CO_2e of C imports and exports assumes all C is released as CO_2. The annual GHG balance for the potato crop was particularly high with a value of 1,669 ± 255 g CO_2e m^{-2} yr^{-1}, which was almost 4 times higher than the value of 401 ± 143 g CO_2e m^{-2} yr^{-1} for the pea crop. Results show that the export of potato tubers and peas accounted for a large proportion of the annual GHG balances (83% and 71%, respectively) (Table 1 and Figure 8). It has been found that a managed highbush blueberry field in the LFV was a net GHG source of 840 ± 126 g CO_2e m^{-2} yr^{-1}, primarily controlled by the application of sawdust mulch (Pow et al., 2020). Ceschia et al. (2010) found that for European croplands, the NEE (through uptake of CO_2), on average, represented 88% of the negative GHG balance, and exported C represented 88% of the positive GHG balance of 203 ± 253 g CO_2e m^{-2} yr^{-1}.

It is important to note that we assumed annual GHG emissions for each crop as pulse emissions to estimate the GHG balances of the three GHGs, and C imports and exports. While we are aware that using values of GWP as opposed to sustained GWP (SGWP) of different GHGs does not provide the actual radiative forcing (Neubauer, 2021), it provides valid information as to whether an ecosystem is a net CO_2e source or sink and compares GHG balances of two different crops.

We would also like to emphasize that impacts of some agricultural management practices and other environmental conditions were not assessed in this study. First, as the need of food is rapidly increasing, herbicides are expected to be used more in crop production globally (Gianessi, 2013). Besides serving as an effective tool to increase crop yield, applying herbicides can change vegetation-soil interactions and consequently alter soil GHG fluxes (Crouzet et al., 2010; Jiang et al., 2015; Oyeogbe et al., 2017). The application of herbicides to an agricultural field (alfalfa) led to largely increased CO_2 emissions which contributed to greater GHG emissions (Shi et al., 2020). Second, the phenological stage of crops can play an important role in GHG fluxes. Vegetation height showed a strong relationship with N_2O fluxes for both peas and maize in a farm in Switzerland, likely because of plant-microorganism competition (Maier et al., 2022).

4. Conclusions

Due to frequent agricultural operations (e.g., herbicide spraying), the field instrumentation system in this study had to be deployed at the edge of the study agricultural field. We combined EC and manual flux chamber measurements with the flux footprint approach to make corrections for the edge effect resulting from the presence of a farm road and a machinery turn-round strip adjacent to the EC tower, and the resultant inhomogeneity of the footprint area, and hence to obtain GHG fluxes for the crop areas. The key findings are summarized as follows:

1. After the flux footprint correction, the potato and pea crops were both weak CO_2 sinks with annual NEE values of -57 ± 9 and -97 ± 16 g C m^{-2} yr^{-1} ($k = 1$), respectively. After taking C export via crop harvest and C import via seeding into account, the potato crop became a C source (NECB = -284 ± 55 g C m^{-2} yr^{-1}), while the pea crop became a weak C sink (NECB = 30 ± 26 g C m^{-2} yr^{-1}).
2. The annual footprint-corrected GHG balances for the potato and pea crops were 417 ± 88 and 152 ± 106 g CO_2e m^{-2} yr^{-1} ($k = 1$), but when including C_{import} and C_{export}, the values were $1{,}699 \pm 255$ and 401 ± 143 g CO_2e m^{-2} yr^{-1}, respectively. For both the potato and the pea crops, N_2O contributed the largest proportion to the annual GHG balances and offset CO_2 uptake from the atmosphere, making both crop fields net GHG sources.
3. R_e and N_2O fluxes after flux footprint corrections were generally higher than those directly measured by EC due to smaller R_e and N_2O fluxes in the edge area compared with the cropped area.
4. Substantial N_2O emissions were triggered by rainfall events during the non-growing season. CH_4 emissions were low and made a small contribution to the GHG balances. The magnitude of R_e mainly followed seasonal changes in T_s. Temporal variations in GPP were closely associated with crop development.

These results highlight the importance of future research into management practices that decrease N_2O emissions and increase C sequestration in agricultural systems. This includes questions about how much can nitrogen fertilizer rates be decreased while maintaining acceptable yields, and the benefits of adding organic amendments such as poultry manure. In agricultural systems like those in this study where the non-growing season is relatively mild and rainfall is high, it will be useful to consider and evaluate how cover crops can be successfully grown during this period and their impacts on C and GHG balances.

Appendix A

A1. Wind Direction Analysis

As shown in Figure A1, f for each landscape component generally followed a uniquely shaped curve closely related to wind direction. However, the f curves varied within a small range for a specific wind direction, which was due to varying atmospheric conditions. It is also apparent that the f curves for the west and the east fields (the left and right panels in Figure A1) exhibited mirror image symmetry due to the EC system being located between the two fields. The highest value of $f_c + f_e$ (0.95) was observed when the wind direction was between 240° and 300°, with f_c (0.6–0.85) being higher and f_e (0–0.35) being lower than those for wind directions outside this range. A similar pattern was observed for the east field with the maximum value of $f_c + f_e$ being approximately 0.92

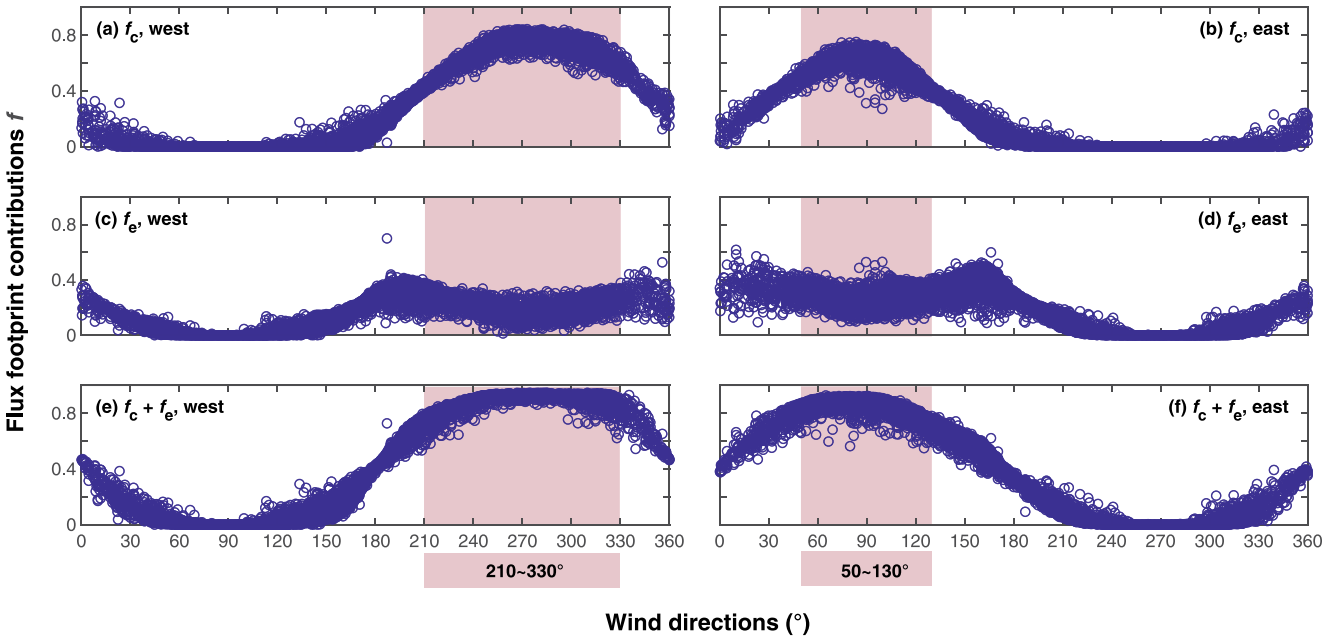

Figure A1. Half-hourly flux footprint contributions (f_c and f_e) during the study period calculated using the two-dimensional Flux Footprint Prediction (FFP) model (Kljun et al., 2015) for the crop area (a and b), edge area (c and d), and the total of the two areas (e and f) for the west and east fields, respectively. The pink colored bars are the two wind-direction ranges selected for filtering the data (CO_2, N_2O, and CH_4 fluxes) for the east and west fields (50–130° and 210–330° for the east and west fields, respectively). In the case of the CH_4 fluxes, it was to minimize the impact from the ditch even though no flux footprint correction was made.

when the wind direction was between 60° and 100°. This suggested that the west-east spans of the crop and the edge areas, both in the west (218 m) and in the east (177 m), were long enough to cover more than 90% of $f_c + f_e$. However, the wind direction range within which the maximum value of $f_c + f_e$ remained high was narrower for the east field than for the west field due to the north-south span of the east field (125 m) being much less than the west field (600 m). In addition, due to the fact that the edge area in the east (14 m) was wider than that in the west (10 m), f_c of the east field was slightly lower (0.5–0.78) while its f_e (0.1–0.4) was higher. Mauder et al. (2013) recommended that a minimum percentage of 70% originating from the target area is required to enable the calculation of flux footprint contributions originating from one or more target areas, and indicated that this threshold can vary depending on the user's requirements. To avoid losing too much data, the threshold was selected as 60% for $f_c + f_e$. Based on this criterion, we decided to filter the data according to the wind direction ranges which are highlighted in pink in Figure A1.

A2. Tarpaulin Experiment

Due to the fact that CO_2 uptake was observed during the non-growing season with the crop field being completely bare soil and the grass in the edge area growing actively, the significant effect of the grass photosynthesis during the non-growing season was confirmed by covering the grass in the edge area near the EC system. In order to provide further insight into the sink strength of the grass during the non-growing season, a 5-day experiment was conducted from 21 to 25 May 2019. The grass immediately to the northwest of the EC system was completely covered by tarpaulins in order to eliminate the effect of grass photosynthesis on EC-measured NEE. Therefore, the sink strength of the grass could be roughly determined by comparing the NEE before and after the tarpaulins were in place using Equation 10. The GPP value of grass was estimated to be between 25 and 40 μmol m^{-2} s^{-1}.

Data Availability Statement

The data set of eddy-covariance, flux-chamber, and biometeorological variables used in this study is available in Zenodo at https://doi.org/10.5281/zenodo.7241474.

Acknowledgments
We gratefully acknowledge the technical support in the field from our research assistants, Brian Wang, Oscar Zimmerman and Chantel Chizen, and the help of our research technician, Jugoslav Kitanovic. We sincerely thank Stan Reynolds and Hugh Reynolds of Reynelda Farm for accommodating our research and their collaboration. We greatly appreciate the help from Eric Leinberger on editing the figures. This work was supported by funding from Agriculture and Agri-Food Canada (Grant AGGP2-036_CA, 2017) and a Natural Sciences and Engineering Research Council (NSERC) Discovery Grant (T.A.B.). Open Access funding enabled and organized by Projekt DEAL.

References

Abdalla, K., Chivenge, P., Ciais, P., & Chaplot, V. (2016). No-tillage lessens soil CO_2 emissions the most under arid and sandy soil conditions: Results from a meta-analysis. *Biogeosciences*, *13*(12), 3619–3633. https://doi.org/10.5194/bg-13-3619-2016

Abdalla, M., Hastings, A., Cheng, K., Yue, Q., Chadwick, D., Espenberg, M., et al. (2019). A critical review of the impacts of cover crops on nitrogen leaching, net greenhouse gas balance and crop productivity. *Global Change Biology*, *25*(8), 2530–2543. https://doi.org/10.1111/gcb.14644

Anthoni, P. M., Knohl, A., Rebmann, C., Freibauer, A., Mund, M., Ziegler, W., et al. (2004). Forest and agricultural land-use-dependent CO_2 exchange in Thuringia, Germany. *Global Change Biology*, *10*(12), 2005–2019. https://doi.org/10.1111/j.1365-2486.2004.00863.x

Asgedom, H., & Kebreab, E. (2011). Beneficial management practices and mitigation of greenhouse gas emissions in the agriculture of the Canadian Prairie: A review. *Agronomy for Sustainable Development*, *31*(3), 433–451. https://doi.org/10.1007/s13593-011-0016-2433–451

Baldocchi, D. (2014). Measuring fluxes of trace gases and energy between ecosystems and the atmosphere—The state and future of the eddy covariance method. *Global Change Biology*, *20*(12), 3600–3609. https://doi.org/10.1111/gcb.12649

Barr, A. G., Black, T. A., Hogg, E. H., Kljun, N., Morgenstern, K., & Nesic, Z. (2004). Inter-annual variability in the leaf area index of a boreal aspen-hazelnut forest in relation to net ecosystem production. *Agricultural and Forest Meteorology*, *126*(3–4), 237–255. https://doi.org/10.1016/j.agrformet.2004.06.011

Bavin, T. K., Griffis, T. J., Baker, J. M., & Venterea, R. T. (2009). Impact of reduced tillage and cover cropping on the greenhouse gas budget of a maize/soybean rotation ecosystem. *Agriculture, Ecosystems & Environment*, *134*(3–4), 234–242. https://doi.org/10.1016/j.agee.2009.07.005

Behnke, G. D., & Villamil, M. B. (2019). Cover crop rotations affect greenhouse gas emissions and crop production in Illinois, USA. *Field Crops Research*, *241*, 107580. https://doi.org/10.1016/j.fcr.2019.107580

Bhandral, R., Bittman, S., Kowalenko, G., Buckley, K., Chantigny, M. H., Hunt, D. E., et al. (2009). Enhancing soil infiltration reduces gaseous emissions and improves N uptake from applied dairy slurry. *Journal of Environmental Quality*, *38*(4), 1372–1382. https://doi.org/10.2134/jeq2008.0287

Bittman, S., & Hunt, D. (2015). Nitrogen management of forages in relation to gaseous emissions – New approaches and considerations. In D. Vijay, M. K. Srivastava, C. K. Gupta, D. R. Malaviya, M. M. Roy, S. K. Mahanta, et al. (Eds.), *Sustainable use of grassland resources for forage production, biodiversity and environmental protection: Proceedings of the 23rd International Grassland Congress. November 20–24, 2015, New Delhi, India* (Vol. 383, pp. 117–128).

British Columbia Agriculture & Food Climate Action Initiative. (2013). Regional adaptation strategies: Delta region. Retrieved from https://www.bcagclimateaction.ca/wp/wp-content/media/RegionalStrategies-Delta.pdf

Canadell, J. G., Monteiro, P. M. S., Costa, M. H., Cotrim da Cunha, L., Cox, P. M., Eliseev, A. V., et al. (Eds.). (2021). *Climate Change 2021: The Physical Science Basis. Contribution of Working Group I to the Sixth Assessment Report of the Intergovernmental Panel on Climate Change* (pp. 673–816). Cambridge University Press. Retrieved from https://www.scopus.com/inward/record.uri?eid=2-s2.0-85116826922&partnerID=40&md5=0e250e3954b81a2fdfe96d7a165c91fd

Ceschia, E., Béziat, P., Dejoux, J. F., Aubinet, M., Bernhofer, C., Bodson, B., et al. (2010). Management effects on net ecosystem carbon and GHG budgets at European crop sites. *Agriculture, Ecosystems & Environment*, *139*(3), 363–383. https://doi.org/10.1016/j.agee.2010.09.020

Chapin, F. S., Woodwell, G. M., Randerson, J. T., Rastetter, E. B., Lovett, G. M., Baldocchi, D. D., et al. (2006). Reconciling carbon-cycle concepts, terminology, and methods. *Ecosystems*, *9*(7), 1041–1050. https://doi.org/10.1007/s10021-005-0105-7

Chen, B., Black, T. A., Coops, N. C., Hilker, T., & Morgenstern, K. (2009). Assessing tower flux footprint climatology and scaling between remotely sensed and eddycovariance measurements. *Boundary-Layer Meteorology*, *130*(2), 137–167. https://doi.org/10.1007/s10546-008-9339-1

Chizen, C. J., Krzic, M., Black, T. A., Jassal, R. S., & Smukler, S. M. (2022). Nitrous oxide emissions from productive and degraded potato fields in the Fraser Valley delta of British Columbia. *Canadian Journal of Soil Science*, *102*(4), 1000–1004. https://doi.org/10.1139/cjss-2022-0032

Christen, A., Jassal, R. S., Black, T. A., Grant, N. J., Hawthorne, I., Johnson, M. S., et al. (2016). Summertime greenhouse gas fluxes from an urban bog undergoing restoration through rewetting. *Mires and Peat*, *18*, 1–24.

Christensen, S., Ambus, P., Arah, J. R. M., Clayton, H., Galle, B., Griffith, D. W. T., et al. (1996). Nitrous oxide emission from an agricultural field: Comparison between measurements by flux chamber and micrometerological techniques. *Atmospheric Environment*, *30*(24), 4183–4190. https://doi.org/10.1016/1352-2310(96)00145-8

Ciais, P., Friedlingstein, P., Friend, A., & Schimel, D. S. (2001). Integrating global models of terrestrial primary productivity. In J. Roy, B. Saugier, & H. A. Mooney (Eds.), *Terrestrial global productivity* (pp. 449–478). Academic Press.

Conrad, R. (2020). Methane production in soil environments—Anaerobic biogeochemistry and microbial life between flooding and desiccation. *Microorganisms*, *8*(6), 881. https://doi.org/10.3390/microorganisms8060881

Crouzet, O., Batisson, I., Besse-Hoggan, P., Bonnemoy, F., Bardot, C., Poly, F., et al. (2010). Response of soil microbial communities to the herbicide mesotrione: A dose-effect microcosm approach. *Soil Biology and Biochemistry*, *42*(2), 193–202. https://doi.org/10.1016/j.soilbio.2009.10.016

Drever, C. R., Cook-Patton, S. C., Akhter, F., Badiou, P. H., Chmura, G. L., Davidson, S. J., et al. (2021). Natural climate solutions for Canada. *Science Advances*, *7*(23), eabd6034. https://doi.org/10.1126/sciadv.abd6034

Ehhalt, D. H., & Schmidt, U. (1978). Sources and sinks of atmospheric methane. *Pure and Applied Geophysics*, *116*(2), 452–464. https://doi.org/10.1007/BF01636899

Environment and Climate Change Canada. (2022). National Inventory Report 1990–2020: Greenhouse Gas Sources and Sinks in Canada: Executive Summary. Retrieved from https://www.canada.ca/en/environment-climate-change/services/climate-change/greenhouse-gas-emissions/inventory.html

Falge, E., Baldocchi, D., Olson, R., Anthoni, P., Aubinet, M., Bernhofer, C., et al. (2001). Gap filling strategies for long term energy flux data sets. *Agricultural and Forest Meteorology*, *107*(1), 71–77. https://doi.org/10.1016/s0168-1923(00)00235-5

Famulari, D., Nemitz, E., Di, C., Phillips, G. J., Thomas, R., House, E., & Fowler, D. (2010). Eddy-covariance measurements of nitrous oxide fluxes above a city. *Agricultural and Forest Meteorology*, *150*(6), 786–793. https://doi.org/10.1016/j.agrformet.2009.08.003

Flessa, H., Ruser, R., Schilling, R., Loftfield, N., Munch, J. C., Kaiser, E. A., & Beese, F. (2002). N_2O and CH_4 fluxes in potato fields: Automated measurement, management effects and temporal variation. *Geoderma*, *105*(3–4), 307–325. https://doi.org/10.1016/S0016-7061(01)00110-0

Forster, P., Storelvmo, T., Armour, K., Collins, W., Dufresne, J. L., Frame, D., et al. (2021). The Earth's energy budget, climate feedbacks, and climate sensitivity. In V. Masson-Delmotte, P. Zhai, A. Pirani, S. L. Connors, C. Péan, S. Berger, et al. (Eds.), *Climate Change 2021: The Physical Science Basis. Contribution of Working Group I to the Sixth Assessment Report of the Intergovernmental Panel on Climate Change* (pp. 923–1054). Cambridge University Press. https://doi.org/10.1017/9781009157896.009

Gianessi, L. P. (2013). The increasing importance of herbicides in worldwide crop production. *Pest Management Science*, *69*(10), 1099–1105. https://doi.org/10.1002/ps.3598

Gillam, K. M., Zebarth, B. J., & Burton, D. L. (2008). Nitrous oxide emissions from denitrification and the partitioning of gaseous losses as affected by nitrate and carbon addition and soil aeration. *Canadian Journal of Soil Science*, *88*(2), 133–143. https://doi.org/10.4141/CJSS06005

Gilmanov, T. G., Aires, L., Barcza, Z., Baron, V. S., Belelli, L., Beringer, J., et al. (2010). Productivity, respiration, and light-response parameters of world grassland and agroecosystems derived from flux-tower measurements. *Rangeland Ecology and Management*, *63*(1), 16–39. https://doi.org/10.2111/REM-D-09-00072.1

Gilmanov, T. G., Baker, J. M., Bernacchi, C. J., Billesbach, D. P., Burba, G. G., Castro, S., et al. (2014). Productivity and carbon dioxide exchange of leguminous crops: Estimates from flux tower measurements. *Agronomy Journal*, *106*(2), 545–559. https://doi.org/10.2134/agronj2013.0270

Gilmanov, T. G., Wylie, B. K., Tieszen, L. L., Meyers, T. P., Baron, V. S., Bernacchi, C. J., et al. (2013). CO_2 uptake and ecophysiological parameters of the grain crops of midcontinent North America: Estimates from flux tower measurements. *Agriculture, Ecosystems & Environment*, *164*, 162–175. https://doi.org/10.1016/j.agee.2012.09.017

Gong, H., Li, J., Liu, Z., Zhang, Y., Hou, R., & Ouyang, Z. (2022). Mitigated greenhouse gas emissions in cropping systems by organic fertilizer and tillage management. *Land*, *11*(7), 1026. https://doi.org/10.3390/land11071026

Hartmann, D. L., Klein Tank, A. M. G., Rusticucci, M., Alexander, L. V., Brönnimann, S., Charabi, Y. A. R., et al. (2013). Observations: Atmosphere and surface. In *Climate Change 2013 the Physical Science Basis: Working Group I Contribution to the Fifth Assessment Report of the Intergovernmental Panel on Climate Change* (Vol. 9781107057999, pp. 159–254). Cambridge University Press. https://doi.org/10.1017/CBO9781107415324.008

Huang, H., Wang, J., Hui, D., Miller, D. R., Bhattarai, S., Dennis, S., et al. (2014). Nitrous oxide emissions from a commercial cornfield (*Zea mays*) measured using the eddy covariance technique. *Atmospheric Chemistry and Physics*, *14*(23), 12839–12854. https://doi.org/10.5194/acp-14-12839-2014

Humphreys, E. R., Black, T. A., Morgenstern, K., Cai, T., Drewitt, G. B., Nesic, Z., & Trofymow, J. A. (2006). Carbon dioxide fluxes in coastal Douglas-fir stands at different stages of development after clearcut harvesting. *Agricultural and Forest Meteorology*, *140*(1–4), 6–22. https://doi.org/10.1016/j.agrformet.2006.03.018

Humphreys, E. R., Black, T. A., Morgenstern, K., Li, Z., & Nesic, Z. (2005). Net ecosystem production of a Douglas-fir stand for 3 years following clearcut harvesting. *Global Change Biology*, *11*(3), 450–464. https://doi.org/10.1111/j.1365-2486.2005.00914.x

Hunt, D. E., Bittman, S., Zhang, H., Bhandral, R., Grant, C. A., & Lemke, R. (2016). Effect of polymer-coated urea on nitrous oxide emission in zero-till and conventionally tilled silage corn. *Canadian Journal of Soil Science*, *96*(1), 12–22. https://doi.org/10.1139/cjss-2015-0071

Hunt, J. E., Laubach, J., Barthel, M., Fraser, A., & Phillips, R. L. (2016). Carbon budgets for an irrigated intensively grazed dairy pasture and an unirrigated winter-grazed pasture. *Biogeosciences*, *13*(10), 2927–2944. https://doi.org/10.5194/bg-13-2927-2016

Jeuffroy, M. H., Baranger, E., Carrouée, B., de Chezelles, E., Gosme, M., Hénault, C., et al. (2013). Nitrous oxide emissions from crop rotations including wheat, oilseed rape and dry peas. *Biogeosciences*, *10*(3), 1787–1797. https://doi.org/10.5194/bg-10-1787-2013

Jiang, J., Chen, L., Sun, Q., Sang, M., & Huang, Y. (2015). Application of herbicides is likely to reduce greenhouse gas (N_2O and CH_4) emissions from rice–wheat cropping systems. *Atmospheric Environment*, *107*, 62–69. https://doi.org/10.1016/j.atmosenv.2015.02.029

Kanianska, R., Jaďuďová, J., Makovníková, J., & Kizeková, M. (2016). Assessment of relationships between earthworms and soil abiotic and biotic factors as a tool in sustainable agricultural. *Sustainability*, *8*(9), 906. https://doi.org/10.3390/su8090906

Kaye, J. P., & Quemada, M. (2017). Using cover crops to mitigate and adapt to climate change. A review. *Agronomy for Sustainable Development*, *37*(1), 1–17. https://doi.org/10.1007/s13593-016-0410-x

Kim, K., Daly, E. J., Flesch, T. K., Coates, T. W., & Hernandez-Ramirez, G. (2022). Carbon and water dynamics of a perennial versus an annual grain crop in temperate agroecosystems. *Agricultural and Forest Meteorology*, *314*, 108805. https://doi.org/10.1016/j.agrformet.2021.108805

Kljun, N., Calanca, P., Rotach, M. W., & Schmid, H. P. (2015). A simple two-dimensional parameterisation for Flux Footprint Prediction (FFP). *Geoscientific Model Development*, *8*(11), 3695–3713. https://doi.org/10.5194/gmd-8-3695-2015

Lee, S. C., Christen, A., Black, A. T., Johnson, M. S., Jassal, R. S., Ketler, R., et al. (2017). Annual greenhouse gas budget for a bog ecosystem undergoing restoration by rewetting. *Biogeosciences*, *14*(11), 2799–2814. https://doi.org/10.5194/bg-14-2799-2017

Levy, P., Drewer, J., Jammet, M., Leeson, S., Friborg, T., Skiba, U., & van Oijen, M. (2020). Inference of spatial heterogeneity in surface fluxes from eddy covariance data: A case study from a subarctic mire ecosystem. *Agricultural and Forest Meteorology*, *280*, 107783. https://doi.org/10.1016/j.agrformet.2019.107783

Liebig, M. A., Morgan, J. A., Reeder, J. D., Ellert, B. H., Gollany, H. T., & Schuman, G. E. (2005). Greenhouse gas contributions and mitigation potential of agricultural practices in northwestern USA and western Canada. *Soil & Tillage Research*, *83*(1), 25–52. https://doi.org/10.1016/j.still.2005.02.008

Lognoul, M., Debacq, A., De Ligne, A., Dumont, B., Manise, T., Bodson, B., et al. (2019). N_2O flux short-term response to temperature and topsoil disturbance in a fertilized crop: An eddy covariance campaign. *Agricultural and Forest Meteorology*, *271*, 193–206. https://doi.org/10.1016/j.agrformet.2019.02.033

Lohila, A., Aurela, M., Regina, K., & Laurila, T. (2003). Soil and total ecosystem respiration in agricultural fields: Effect of soil and crop type. *Plant and Soil*, *251*(2), 303–317. https://doi.org/10.1023/A:1023004205844

Luttmerding, H. A. (1981). *Soils of the Langley-Vancouver Map Area. RAB Bulletin* (Vol. 18, p. 227). BC Ministry of Environment. Map 6.

Lv, F., Song, J., Giltrap, D., Feng, Y., Yang, X., & Zhang, S. (2020). Crop yield and N_2O emission affected by long-term organic manure substitution fertilizer under winter wheat-summer maize cropping system. *Science of the Total Environment*, *732*, 139321. https://doi.org/10.1016/j.scitotenv.2020.139321

Ma, R., Yu, K., Xiao, S., Liu, S., Ciais, P., & Zou, J. (2022). Data-driven estimates of fertilizer-induced soil NH_3, NO and N_2O emissions from croplands in China and their climate change impacts. *Global Change Biolology*, *28*(3), 1008–1022. https://doi.org/10.1111/gcb.15975

Maier, R., Hörtnagl, L., & Buchmann, N. (2022). Greenhouse gas fluxes (CO_2, N_2O and CH_4) of pea and maize during two cropping seasons: Drivers, budgets, and emission factors for nitrous oxide. *Science of the Total Environment*, *849*, 157541. https://doi.org/10.1016/j.scitotenv.2022.157541

Mauder, M., Cuntz, M., Drüe, C., Graf, A., Rebmann, C., Schmid, H. P., et al. (2013). A strategy for quality and uncertainty assessment of long-term eddy-covariance measurements. *Agricultural and Forest Meteorology*, *169*, 122–135. https://doi.org/10.1016/j.agrformet.2012.09.006

Merbold, L., Decock, C., Eugster, W., Fuchs, K., Wolf, B., Buchmann, N., & Hörtnagl, L. (2021). Are there memory effects on greenhouse gas emissions (CO_2, N_2O and CH_4) following grassland restoration? *Biogeosciences*, *18*(4), 1481–1498. https://doi.org/10.5194/bg-18-1481-2021

Molodovskaya, M., Warland, J., Richards, B. K., Öberg, G., & Steenhuis, T. S. (2011). Nitrous oxide from heterogeneous agricultural landscapes: Source contribution analysis by eddy covariance and chambers. *Soil Science Society of America Journal*, *75*(5), 1829–1838. https://doi.org/10.2136/sssaj2010.0415

Montagnani, L., Grünwald, T., Kowalski, A., Mammarella, I., Merbold, L., Metzger, S., et al. (2018). Estimating the storage term in eddy covariance measurements: The ICOS methodology. *International Agrophysics*, *32*(4), 551–567. https://doi.org/10.1515/intag-2017-0037

Nagy, W., Berninger, V. W., & Abbott, R. D. (2006). Contributions of morphology beyond phonology to literacy outcomes of upper elementary and middle-school students. *Journal of Educational Psychology*, *98*(1), 134–147. https://doi.org/10.1037/0022-0663.98.1.134

Needelman, B. A., Kleinman, P. J., Strock, J. S., & Allen, A. L. (2007). Drainage ditches: Improved management of agricultural drainage ditches for water quality protection: An overview. *Journal of Soil and Water Conservation*, *62*(4), 171–178.

Nemitz, E., Mammarella, I., Ibrom, A., Aurela, M., Burba, G. G., Dengel, S., et al. (2018). Standardisation of eddy-covariance flux measurements of methane and nitrous oxide. *International Agrophysics*, *32*(4), 517–549. https://doi.org/10.1515/intag-2017-0042

Neubauer, S. C. (2021). Global warming potential is not an ecosystem property. *Ecosystems*, *24*, (8), 1–11. https://doi.org/10.1007/s10021-021-00631-x

Nielsen, U. N., & Ball, B. A. (2015). Impacts of altered precipitation regimes on soil communities and biogeochemistry in arid and semi-arid ecosystems. *Global Change Biology*, *21*(4), 1407–1421. https://doi.org/10.1111/gcb.12789

Oyeogbe, A. I., Das, T. K., Bhatia, A., & Singh, S. B. (2017). Adaptive nitrogen and integrated weed management in conservation agriculture: Impacts on agronomic productivity, greenhouse gas emissions, and herbicide residues. *Environmental Monitoring and Assessment*, *189*(4), 1–11. https://doi.org/10.1007/s10661-017-5917-3

Patel, N. R., Pokhariyal, S., Chauhan, P., & Dadhwal, V. K. (2021). Dynamics of CO_2 fluxes and controlling environmental factors in sugarcane (C4)–wheat (C3) ecosystem of dry sub-humid region in India. *International Journal of Biometeorology*, *65*(7), 1069–1084. https://doi.org/10.1007/s00484-021-02088-y

Pattey, E., Blackburn, L. G., Strachan, I. B., Desjardins, R., & Dow, D. (2008). Spring thaw and growing season N_2O emissions from a field planted with edible peas and a cover crop. *Canadian Journal of Soil Science*, *88*(2), 241–249. https://doi.org/10.4141/CJSS06035

Peacock, M., Audet, J., Bastviken, D., Futter, M. N., Gauci, V., Grinham, A., et al. (2021). Global importance of methane emissions from drainage ditches and canals. *Environmental Research Letters*, *16*(4), 044010. https://doi.org/10.1088/1748-9326/abeb36

Phillips, R., Griffith, D. W., Dijkstra, F., Lugg, G., Lawrie, R., & Macdonald, B. (2013). Tracking short-term effects of nitrogen-15 addition on nitrous oxide fluxes using Fourier-transform infrared spectroscopy. *Journal of Environmental Quality*, *42*(5), 1327–1340. https://doi.org/10.2134/jeq2013.02.0067

Pihlatie, M., Syväsalo, E., Simojoki, A., Esala, M., & Regina, K. (2004). Contribution of nitrification and denitrification to N_2O production in peat, clay and loamy sand soils under different soil moisture conditions. *Nutrient Cycling in Agroecosystems*, *70*(2), 135–141. https://doi.org/10.1023/B:FRES.0000048475.81211.3c

Pow, P., Black, T. A., Jassal, R. S., Nesic, Z., Johnson, M., Smukler, S., & Krizc, M. (2020). Greenhouse gas exchange over a conventionally managed highbush blueberry field in the Lower Fraser Valley in British Columbia, Canada. *Agricultural and Forest Meteorology*, *295*, 108152. https://doi.org/10.1016/j.agrformet.2020.108152

Rochette, P., Liang, C., Pelster, D., Bergeron, O., Lemke, R., Kroebel, R., et al. (2018). Agriculture, ecosystems and environment soil nitrous oxide emissions from agricultural soils in Canada: Exploring relationships with soil, crop and climatic variables. *Agriculture, Ecosystems & Environment*, *254*, 69–81. https://doi.org/10.1016/j.agee.2017.10.021

Saarnio, S., Heimonen, K., & Kettunen, R. (2013). Biochar addition indirectly affects N_2O emissions via soil moisture and plant N uptake. *Soil Biology and Biochemistry*, *58*, 99–106. https://doi.org/10.1016/j.soilbio.2012.10.035

Saunois, M., Stavert, A. R., Poulter, B., Bousquet, P., Canadell, J. G., Jackson, R. B., et al. (2020). The global methane budget 2000–2017. *Earth System Science Data*, *12*(3), 1561–1623. https://doi.org/10.5194/essd-12-1561-2020

Schaufler, G., Kitzler, B., Schindlbacher, A., Skiba, U., Sutton, M. A., & Zechmeister-Boltenstern, S. (2010). Greenhouse gas emissions from European soils under different land use: Effects of soil moisture and temperature. *European Journal of Soil Science*, *61*(5), 683–696. https://doi.org/10.1111/j.1365-2389.2010.01277.x

Schiller, C. L., & Hastie, D. R. (1994). Exchange of nitrous oxide within the Hudson Bay lowland. *Journal of Geophysical Research*, *99*(D1), 1573. https://doi.org/10.1029/93jd01358

Schmid, H. P. (1994). Source areas for scalars and scalar fluxes. *Boundary-Layer Meteorology*, *67*(3), 293–318. https://doi.org/10.1007/BF00713146

Schrier-Uijl, A. P., Kroon, P. S., Hensen, A., Leffelaar, P. A., Berendse, F., & Veenendaal, E. M. (2010). Comparison of chamber and eddy covariance-based CO_2 and CH_4 emission estimates in a heterogeneous grass ecosystem on peat. *Agricultural and Forest Meteorology*, *150*(6), 825–831. https://doi.org/10.1016/j.agrformet.2009.11.007

Seneviratne, S., Nicholls, N., Easterling, D., Goodess, C., Kanae, S., Kossin, J., et al. (2012). Changes in climate extremes and their impacts on the natural physical environment. Chapter 3 of Managing the Risks of Extreme Events and Disasters to Advance Climate Change Adaptation. A Special Report of Working Groups I and II of the Intergovernmental Panel on Climate Change (IPCC).

Shcherbak, I., Millar, N., & Robertson, G. P. (2014). Global metaanalysis of the nonlinear response of soil nitrous oxide (N_2O) emissions to fertilizer nitrogen. *Proceedings of the National Academy of Sciences*, *111*(25), 9199–9204. https://doi.org/10.1073/pnas.1322434111

Sheehy, J. E., & Peacock, J. M. (1975). Canopy photosynthesis and crop growth rate of eight temperate forage grasses. *Journal of Experimental Botany*, *26*(5), 679–691. https://doi.org/10.1093/jxb/26.5.679

Shi, L., Guo, Y., Ning, J., Lou, S., & Hou, F. (2020). Herbicide applications increase greenhouse gas emissions of alfalfa pasture in the inland arid region of northwest China. *PeerJ*, *8*, e9231. https://doi.org/10.7717/peerj.9231

Smith, K. A., McTaggart, I. P., & Tsuruta, H. (1997). Emissions of N_2O and NO associated with nitrogen fertilization in intensive agriculture, and the potential for mitigation. *Soil Use and Management*, *13*(S4), 296–304. https://doi.org/10.1111/j.1475-2743.1997.tb00601.x

Song, Y., Jiao, W., Wang, J., & Wang, L. (2022). Increased global vegetation productivity despite rising atmospheric dryness over the last two decades. *Earth's Future*, *10*(7), e2021EF002634. https://doi.org/10.1029/2021EF002634

Statistics Canada. (2016). Census of agriculture. *Land and crops*.

Suleau, M., Moureaux, C., Dufranne, D., Buysse, P., Bodson, B., Destain, J. P., et al. (2011). Respiration of three Belgian crops: Partitioning of total ecosystem respiration in its heterotrophic, above- and below-ground autotrophic components. *Agricultural and Forest Meteorology*, *151*(5), 633–643. https://doi.org/10.1016/j.agrformet.2011.01.012

Thilakarathna, S. K., Konschuh, M., Woods, S. A., & Hernandez-Ramirez, G. (2023). Nitrous oxide emissions and productivity of irrigated potato: Effects of nitrogen fertilization options. *Agronomy Journal*, *115*(1), 161–180. https://doi.org/10.1002/agj2.21213

Tiedje, J., Sexstone, A., Parkin, T., & Revsbech, N. (1984). Anaerobic processes in soil. *Plant and Soil*, *76*(1–3), 197–212. https://doi.org/10.1007/bf02

Tilman, D., Balzer, C., Hill, J., Befort, B. L., Tilman, D., Balzerb, C., et al. (2011). Global food demand and the sustainable intensification of agriculture. *Proceedings of the National Academy of Sciences of the United States of America*, *108*(50), 20260–20264. https://doi.org/10.1073/pnas.1116437108

Tribouillois, H., Constantin, J., & Justes, E. (2018). Cover crops mitigate direct greenhouse gases balance but reduce drainage under climate change scenarios in temperate climate with dry summers. *Global Change Biology*, *24*(6), 2513–2529. https://doi.org/10.1111/gcb.14091

van Dijk, M., Morley, T., Rau, M. L., & Saghai, Y. (2021). A meta-analysis of projected global food demand and population at risk of hunger for the period 2010–2050. *Nature Food*, *2*(7), 494–501. https://doi.org/10.1038/s43016-021-00322-9

Wagner-Riddle, C., Furon, A., Mclaughlin, N. L., Lee, I., Barbeau, J., Jayasundara, S., et al. (2007). Intensive measurement of nitrous oxide emissions from a corn-soybean-wheat rotation under two contrasting management systems over 5 years. *Global Change Biology*, *13*(8), 1722–1736. https://doi.org/10.1111/j.1365-2486.2007.01388.x

Waldo, S., Chi, J., Pressley, S. N., O'Keeffe, P., Pan, W. L., Brooks, E. S., et al. (2016). Assessing carbon dynamics at high and low rainfall agricultural sites in the inland Pacific Northwest US using the eddy covariance method. *Agricultural and Forest Meteorology*, *218–219*, 25–36. https://doi.org/10.1016/j.agrformet.2015.11.018

Waldo, S., Russell, E. S., Kostyanovsky, K., Pressley, S. N., O'Keeffe, P. T., Huggins, D. R., et al. (2019). N_2O emissions from two agroecosystems: High spatial variability and long pulses observed using static chambers and the flux-gradient technique. *Journal of Geophysical Research: Biogeosciences*, *124*(7), 1887–1904. https://doi.org/10.1029/2019JG005032

Wang, L., Wang, C., Pan, Z., Xu, H., Gao, L., Zhao, P., et al. (2017). N_2O emission characteristics and its affecting factors in rain-fed potato fields in Wuchuan County, China. *International Journal of Biometeorology*, *61*(5), 911–919. https://doi.org/10.1007/s00484-016-1271-3

Webb, E. K., Pearman, G. I., & Leuning, R. (1980). Correction of flux measurements for density effects due to heat and water vapour transfer. *Quarterly Journal of the Royal Meteorological Society*, *106*(447), 85–100. https://doi.org/10.1002/qj.49710644707

Wiesner, S., Duff, A. J., Niemann, K., Desai, A. R., Crews, T. E., Risso, V. P., et al. (2022). Growing season carbon dynamics differ in intermediate wheatgrass monoculture versus biculture with red clover. *Agricultural and Forest Meteorology*, *323*, 109062. https://doi.org/10.1016/j.agrformet.2022.109062

Wu, L. F., Li, B. B., Qin, Y., & Gregorich, E. (2017). Soil CO_2 emission and carbon budget of a wheat/maize annual double-cropped system in response to tillage and residue management in the North China Plain. *International Journal of Agricultural Sustainability*, *15*(3), 253–263. https://doi.org/10.1080/14735903.2017.1288518